1239

key words:
1- bracing buildings
2- cyclic loading
3- earthquake testing

Department of Civil Engineering

The University of Michigan
College of Engineering

Ann Arbor, Michigan 48109

December 1987 Research Report UMCE 87-8

EFFECT OF STITCH SPACING ON THE CYCLIC BEHAVIOR OF BUILT-UP BRACING MEMBERS

(DOUBLE ANGLE AND DOUBLE CHANNEL SECTIONS)

Farhang Aslani
Subhash C. Goel main author
Peixin Xu

A Report on Research Sponsored by
American Institute of Steel Construction

Department of Civil Engineering
The University of Michigan
College of Engineering

Ann Arbor Michigan 48109

TABLE OF CONTENTS

Department of Civil Engineering

2340 G. G. Brown Building
Ann Arbor, Michigan 48109-2125
313/764-8495

College of Engineering
The University of Michigan

December 2, 1987

Mr. Nestor Iwankiw
Assistant Director of Engineering
AISC
400 N. Michigan Avenue
Chicago, IL 60611-4185

Dear Nestor:

Our report which describes the results obtained during the first year effort on the research project is completed. I am enclosing 5 copies of this report for your use. As I mentioned to you a couple of weeks ago, we have not arrive at specific conclusions or recommendations at this stage. The proposed work for the second year when combined with the results obtained thus far will result in a final report next year in which I expect to see real specific design recommendations based on experimental data as well as analysis. Nevertheless, the results presented in this report are very interesting as well as useful. We printed 30 copies of this report and I plan to mail it to most of the leading researchers and practitioners who are interested in this topic. I expect to print more copies and do broader publicity of the final report next year.

Please let me know if you have any comments regarding this report or if you need additional copies. Your support last year for our work on this topic is greatly appreciated. I am confident that the requested support this year will bring our study to a most fruitful conclusion.

With best regards.

Sincerely,

Subhash C. Goel

Subhash C. Goel
Professor

Encl.

1 INTRODUCTION

1.1 Problem Statement

The use of braced steel frames in seismic-resistant design is quite popular, mainly because of a higher stiffness-to-cost ratio as compared to the moment-resisting frames. It is less economical to use moment frames to resist lateral loads along the weak direction of a building. Survival of a braced structure during a severe earthquake strongly depends on the ductility and energy dissipation capacity of the braces. During a severe earthquake the lateral deflections of the frame cause the braces to buckle and stretch alternately. High dependence of a braced frame performance on the cyclic behavior of the braces has attracted attention of some investigators during recent years. Some of these investigations have been conducted in full scale [1,2,5,6,7], and have provided insight into the seismic behavior of the braces and braced structures.

Built-up sections have not received much attention of the researchers despite their widespread use in practice, thus, raising questions concerning their general performance and stitching requirements in particular. In current design practice the stitches are spaced such that the individual elements of the member will not buckle before the overall member. To meet this condition, AISC Specification [14] Section 1.18.2.4 requires that the slenderness ratio of the individual components between stitches shall not exceed that of the built-up member. There is no strength requirement for stitches in general, except for lacing bars, which are designed for 2% of the axial compressive force. Therefore, the strength of stitches is generally provided at a nominal level. The current Canadian specification CSA Standard S16-19569 has a similar requirement, while in its 1961 edition the requirement was more stringent, limiting the slenderness ratio of the individual components to 75% of that of the built-up member and suggesting a maximum spacing of 24" between stitches. British Specification BS 449-1970 in Sections 30, 36, and 37 limits the individual slenderness ratio to 60% of that of the built-up member but not to exceed 40. The German Specification DIN-4114 1952, in Sections 8.213, 8.22, and 8.36, limits the individual slenderness ratio to 50 but does not relate it to the slenderness ratio of the overall member.

A previous study by Astaneh, Goel, and Hanson [2] on stitched double angle bracing members has shown that stitches as per current design practice serve their intended purpose up to the point of the first buckling load only, i.e., the individual elements do not buckle before the buckling load

of the overall member is achieved. This requirement essentially applies to the case of monotonic loading. Under cyclic loading, however, it is necessary to investigate if this requirement is adequate to ensure satisfactory performance. Satisfactory performance includes a ductile behavior with stable hysteresis loops. Thus, in this investigation the adequacy of this requirement is studied and attempt is made to establish criteria which ensures adequate ductility and energy dissipation capacity.

When an out-of-plane buckling member continues to deform in the post-buckling region, a plastic hinge forms in the member at a point some distance from the mid length which has smaller section modulus compared to the mid length if a stitch is provided there. The spacing of the stitches is not close enough to prevent plastic bending of the individual components of the section, as is evident in Figure 1.1 from the closing of the gap between the two angles. When a stitch is not provided at mid length this closing of the gap occurs at mid length. This gap closing, which is due to the individual component bending, has at least four recognizable disadvantages as follows:

1 The convex-side component in subsequent tension cycles does not become fully straight, as seen in Figure 1.2. Consequently, at mid length most tension load is carried by the other component leading to decrease in its fracture life. This becomes worse in case of a large b/t ratio in which local buckling causes most tension load to be carried by only 1/4 of the total section, i.e., the back-to-back leg of the convex-side component.

2 The above phenomenon also leads to reduction in buckling loads in subsequent cycles since it causes the load to be carried mostly by the component which remains relatively straight.

3 Another adverse effect of tension load transfer from one component to the other is that this transfer is through a nominally designed stitch, which is not strong enough for such a force transfer, resulting in very early failure. Such failure of stitches was reported by Astaneh [2] and Popov [5].

4 At the beginning of the post-buckling range, zone C-D in Figure 1.3, the convex-side component contributes most of the resistance to the P- Δ effect because of its greater relative straightness. The increase in axial deformation in zone D-E in Figure 1.3 causes complete gap closing which allows contribution from both components **but with a smaller overall plastic section modulus compared to the virgin specimen**. This, besides the geometric effect, may be another reason for reduction of the slope of hysteresis loop in this region as the axial deformation increases. Greater slope of the hysteresis loop in the post-buckling range means greater drop in the capacity of the member to sustain axial load. Nevertheless, pinching in the hysteresis loop in the post-buckling region occurs due to the larger slope of hysteresis loop at the beginning of the post-buckling range, and also due to the reduced overall plastic section modulus in zone D-E .

It should be noted that the closing of the gap is inevitable due to tendency of the individual components to bending about their own weak axis, while being subjected to large axial and

consequently lateral deformation in post-buckling region. However, **closer stitch spacing can delay this adverse gap-closing phenomenon until a much larger level of lateral deformation which occurs during a rather severe deformation history**. Thus, current code provision for stitch spacing is not adequate for built-up sections to develop full fracture life, full buckling load in subsequent cycles, and full moment capacity to resist the P-Δ effect. These result in a significant loss of energy dissipation capacity of the member under cyclic loading.

1.2 Related Literature

The behavior of braced frames and bracing members subjected to severe earthquake excitations has been extensively studied in recent years both experimentally and analytically. The excitations caused by earthquake ground motion are dynamic in nature. The adoption of the quasi-static method is due to the complexity of simulating dynamic excitations in the laboratory and the difficulties in observing fine details of the behavior during such excitation. The quasi-static method will be used in this study as well. To investigate the correlation of hysteresis response between quasi-static and dynamic tests, Kahn and Hanson [10] performed a series of cyclic experimental tests on 1 in. by 1/2 in. steel bars with the slenderness ratio varying from 85 to 210. The bars were tested under dynamic and quasi-static loading conditions. It was found that dynamic hysteresis response was nearly identical to the quasi-static response, although the responses were slightly different when the brace was loaded in tension.

Black, Wenger, and Popov [5] reported the results of four full-scale tests of double angle struts subjected to axial cyclic loading. The tests were part of an experimental program on cyclic behavior of various structural shapes such as wide flanges, tubes, tees, and double angles. Two distinctive end conditions were employed. Specimens had either both ends pinned or one pinned and the other fixed. Two major conclusions from their report are quoted here:

1 The conventional definition of the effective slenderness ratio deduced on an elastic basis carries over into the inelastic range.

2 Stitching of built-up members as currently specified in standard codes (AISC) is unconservative in the case of severe load reversals.

Astaneh, Goel, and Hanson, [1] and [2], studied the behavior of stitched double-angle bracing members for both in-plane and out-of-plane buckling. The latter will be briefly discussed here since it is related to, or better to say the basis for, the present study. Three bolted and six welded

specimens were tested, all of them designed to buckle out of plane . Since the main emphasis was on behavior of connections and stitches, different stitch spacing effect was not investigated but suggested for future investigation. The following conclusions and recommendation were drawn with respect to out-of-plane buckling double-angle bracing members:

1 The stitch spacing according to Section 1.18.2.4 of the AISC Specification [14] is adequate to prevent single-angle buckling between the stitches before the overall buckling of the bracing member **but not enough to prevent individual plastic bending and the gap closing in the post-buckling range.**

2 The behavior of stitches and end gusset plates has important effect on the overall ductility and cyclic behavior of the out-of-plane buckling double-angle bracing members. Current practice does not ensure the ductility of connections subjected to cyclic loading.

3 In all specimens, two plastic hinges formed in the gusset plate at the ends and one plastic hinge formed at mid span. The deformed shape of test specimen after buckling is similar to the deformed shape of an axially loaded compression member with hinged-end connection suggesting an effective length factor close to 1.

4 The first buckling load of all specimens is close to the value calculated from Eqs. 1.5-1 and 1.5-2 of the AISC Specification [14] without using the factor of safety.

5 The buckling load capacity of the bracing members decreases significantly from the first to the second cycle, and continues to decrease at a smaller rate throughout cyclic loading. This is due to Baushinger effect and also residual curvature caused by post-buckling lateral deformations in previous cycles.

6 Local buckling occurs in the outstanding legs. The b/t ratio of **outstanding leg** should not exceed the limits permitted in Section 2.7 of the AISC Specification [14].

7 The forces transferred by stitches in out-of-plane buckling bracing members can be large. The nominal stitches cannot withstand severe cyclic deformations. The stitches in out-of-plane buckling member should be designed to transfer a force at least equal to 1/4 total yield capacity of the member. The force should be assumed to act along the centroidal axis of the individual angles.

8 The gusset plates designed according to current practice generally showed poor ductility and early fracture. An adequate free length of gusset plate beyond the angle is necessary to ensure free formation of plastic hinges and to improve ductility of the gusset plates. A minimum free length equal to **twice the thickness of the gusset plate** proved to be adequate while excessive free length creates the possibility of buckling of the gusset plate by itself.

El-Tayem and Goel [6] studied the cyclic behavior of angle X-bracing members in full-scale tests. They concluded the following:

1 The design of X-bracing systems can be based on the buckling strength of the compression diagonal over half length.

2 Width-Thickness ratio should be lower than what is commonly specified in allowable stress design

procedure.

3 Local Buckling is more severe in the case of out -out-of-plane buckling members.

In the analytical domain, modeling the hysteresis behavior of bracing members has been the center of focus. Popov, Takanashi, and Roeder [12] in their report gave a brief summary of the models proposed prior to 1976. Later, simple models were proposed by Singh [13] and later modified by Jain, Goel, and Hanson [8]. Ballio, Gobetti, and Zanon [3] proposed an empirical model to predict the cyclic behavior of double angle bracings. The model is based on the data obtained by Zanon from his monotonic tests of small scale specimens.

1.3 Objectives and Scope of Research

The purpose of this investigation is to analyze the effect of stitch spacing on the performance of built-up double angle and double channel bracing members under cyclic loading. The analysis is based on previous tests by Astaneh and Goel [2] supplemented by five additional tests on double angle and three on double channel specimens. Also, the interaction of stitch spacing with another critical parameter, width-thickness ratio, is investigated. First, a specimen was tested which had stitches according to the current recommendation of AISC Specification [14] . Then, for the next specimens, modifications in the number of stitches and width-thickness ratio were implemented, based on data analysis and the observed behavior of the previous specimen. Tests in this study were performed only on welded members, since the behavior of bolted specimens has been found to be inferior due to slippage and weakening of the section by holes.

The experimental program is described in Chapter 2 and the test results are discussed in Chapter 3. Chapter 4 gives the summary and conclusions and finally Chapter 5 contains suggestions for future study based on the observations and conclusions of the present study.

2 EXPERIMENTAL PROGRAM

2.1 Test program

The experimental program consisted of testing five double angle and three double channel full size specimens under quasi-static cyclic loading. The test specimens represent double angle and double channel bracing members in a steel frame. The end connections of the bracing members use welded gusset plates.

2.1.1 Double Angle Specimens

All five double angle specimens were made from two unequal leg angles with longer legs placed back to back. This configuration is the conventional one used in practice in which the angles are stitched together and connected to the gusset plate by fillet weld. The five specimens tested fall into two categories of width-thickness ratio i.e., 10 and 6.7. Other geometric properties of the specimens are given in Table 2.1. Four different stitch spacings were employed, of which the first one was selected according to AISC Specification [14] to evaluate the current design practice. Decisions on the stitch spacing of subsequent specimens were based on the test observation of this specimen.

2.1.2 Double Channel Specimens

The three double channel specimens tested were made from two channel sections placed toe-to-toe to form a box section since this configuration is the most efficient utilization of the material. Two American standard channel sections were selected giving a slenderness ratio of about 50 and width-thickness ratios of the channel web of approximately 14 and 18. Other geometric properties of the test specimens are given in Table 2.2. Three different stitch spacings were employed, all in compliance with AISC Specifications to prevent buckling of the individual components before the overall buckling of the member under compression.

2.2 Test Set-Up

2.2.1 Four-Hinged frame

The loading system shown in Figure 2.1 consists of a four-hinged testing frame and a double acting hydraulic actuator. The specimens were diagonally mounted in the four-hinged frame consisting of two horizontal beams of W53X142 and two vertical columns of W14X53. The beams and columns are connected by four 3-1/2 inch pins. At the location of the pins additional reinforcing

and stiffening plates are used. The lower beam of the four-hinged frame is fixed to the supporting structural floor, but the upper beam is free to move horizontally in its own plane. The hydraulic actuator forces the vertical columns of the four-hinged frame to rotate about base hinges while restricting the out-of-plane plane movement of the test frame.

2.2.2 Hydraulic Actuator System

The loading system consists of a double-acting hydraulic actuator Model 207.16a manufactured by MTS systems corporation. The push-pull hydraulic actuator is positioned horizontally directly above the top beam of the four-hinged frame. The fixed and active ends of the actuator are connected to the reaction wall and to a bracket attached to the upper beam of the four-hinged frame, respectively. A universal alignment mounting accessory, swivel base and heads, is used at each end of the actuator in order to reduce misalignment due to deformations of the test frame during the test and provide pivotal freedom at the ends. The actuator has a double acting piston with a capacity of 246 kips (1.1 MN) in tension and 328 kips (1.4 MN) in compression and a maximum stroke length of 16 inches (41 cm.).

The pressurized oil needed for the actuator is provided by a 506.61-70-gpm hydraulic pump by MTS systems corporation. The movement of the piston is controlled by a servovalve unit, mounted on the actuator manifold, which is controlled either manually or automatically by a 406.11 model controller by MTS systems corporation. All the tests in this program were carried out by manual control because of need for stopping the operation at any desired point in order to inspect specimens , to make recordings, and to take photographs.

The loading system performed well during the tests except for two cases in which, due to improper functioning of the control system, the first cycle buckling loads of specimens A2 and A3 were not recorded. In order to keep the loading system in good shape, the actuator was exercised for many hours before mounting a specimen in the test frame.

2.2.3 Instrumentation

The instrumentation shown schematically in Fig. 2.2 consists of the followings:

1 Two Linear Variable Differential Transducers (LVDT) for measuring axial deformations;
2 Ruler for lateral deformation measurements;
3 Load cell for axial load measurement (not shown in the schematic);
4 EP series strain gages for strain measurement at critical points.

LVDT's measured the deformations between the two moving parts of the telescopic tubes which were connected to the end plates of a specimen. Considerable differences between the two measurements were recorded. It can be attributed mainly to rotation of the end plates, therefore the average of the two measurements was used to define the axial deformation of specimens.

The wire transducer used in previous tests at The University of Michigan for measurement of lateral deformation gave incorrect values. Therefore, a simple ruler was used to measure the lateral displacement at mid span of the specimens.

The load cell measured the horizontal force applied by the actuator to the upper beam of the four-hinged frame. Neglecting some small friction force in the hinges of the frame as well as some small geometric change, the axial force in the specimen can be linearly related to the force measured by the load cell. The test specimens were positioned diagonally in the four-hinged frame, making about a 45 degree angle with horizontal beams of the frame. The actuator applied the force to the upper beam in the horizontal direction, so the axial force in the specimen would be equal to the force applied by the actuator divided by (Cos 45^{o}).

Sixteen to twenty four EP series straingages were placed over the surface of each specimen at two or three predesignated critical locations in order to cross-check the output of the load cell unit and to possibly use the recorded strains in the analysis of the post-buckling bending.

2.2.4 Data Acquisition System

The data acquisition system, Fig. 2.3, consists of the following components:

1 **X-Y Recorder :** A Hewlete Packard X-Y Recorder, Model HP 7015B, is used to plot the hysteresis loops during the tests. It is very useful to check the rod transducers performance and to visually observe phenomena such as overall buckling and yielding in the members.

2 **Data Channel Scanner :** A Hewlete Packard data acquisition system, Model HP 3497A, is used to scan the channels during the tests. The data is stored on a cassette tape and portions of the data are printed as desired.

3 **Voltmeters:** A digital voltmeter is used to monitor and control the voltage changes of the load cell which represents the direction and magnitude of the axial deformation.

2.2.5 Data Processing System

A few computer programs were developed to store the data on the HP computer tape. The programs converted the data recorded as voltage into appropriate physical quantities by applying corresponding calibration factors. A computer program, "PCTALK", was used to transfer the data

from the HP computer to an IBM computer and a few computer programs were developed to process the acquired data.

2.3 Selection of Test Specimens

2.3.1 Double Angle Specimens

Due to single axis of symmetry in the cross section, double angle members could buckle in one of three modes; in-plane flexural, out-of-plane flexural, and torsional flexural. All specimens were designed to buckle in out-of-plane flexural mode, and they did so. Two sets of angles, 2L2.5x3.5x1/4 and 2L2.5x3.5x3/8, were selected which give effective slenderness ratios of 130 and 117, respectively. Two different stitch spacings were used for the first set and three different stitch spacings were used for the second. The slenderness ratios were calculated based on Ky=1 since the buckling shape was very close to that of a hinged-end axially-loaded strut. This stems from the very small out-of-plane stiffness of the gusset plate compared to that of the member. The difference in the slenderness ratio is due to selection of two different width-thickness ratios of 10 and 6.7. Different width-thickness ratios and slenderness ratios were selected in order to examine their effects on the stitch spacing requirement. Details of all specimens are shown in Figure 2.4 through 2.8.

2.3.2 Double Channel Specimens

Channel sections were welded toe-to-toe to form a box section, as shown in Figure 2.9. This configuration is used in some countries for bracing members and found to be very promising. First, cold-formed box sections exhibit poor ductile behavior due to their short fracture life. However, a box section made from A36 double channels has the desirable characteristics of a box section while it is not cold-formed, leading to more ductile behavior. Second, large thickness of the channel flanges results in smaller width-thickness ratio of the sides of the box section which reduces the severity of local buckling in the post-buckling range. Nevertheless, the behavior of this kind of built-up section has not yet been studied well.

Two American standard channels , C5x6.7 and C4x5.4 were used with a special end connection as shown in Figure 2.10. This end connection was designed to provide a fixed-end connection, against both in-plane and out-of-plane buckling. This arrangement decreases the slenderness ratio, and consequently increases the buckling loads. Thus, an effective length factor of 0.5 was used in all calculations, i.e., $K_x=K_y= 0.5$.

2.4 Design Philosophy

Two philosophies can generally be used in the design of the connections for bracing members. In the first philosophy, the connections are designed to develop the tension yield capacity of the member. In the second philosophy, the connections are designed without the one-third increase usually permitted for stresses in members resulting from earthquake forces. These two design philosophies are usually referred to as "Ultimate strength design" and "Allowable stress design", respectively. Both of these philosophies satisfy the requirement of Section 2312(j)1G of the 1982 edition of the Uniform Building Code (UBC). The allowable stress philosophy was used in this study, in which the connections were designed to resist a tension force equal to 1.33 times the allowable tension capacity of the bracing member using the provisions of Part 1 of the AISC Specification [14]. As a result, the tension capacity of the connections was 33% more than that of the bracing members. A detailed design method for gusset plates as recommended by Astaneh [2] was followed to ensure having a ductile behavior of the connections. The most important recommendation in the Astaneh's method, i.e., "An adequate free length of gusset plate equal to twice its thickness beyond the angle is necessary to ensure the free formation of a plastic hinge and to improve ductility of the gusset plate", proved to be adequate to prevent failure in the connections.

2.5 Fabrication of The Specimens

The following steps were taken in the fabrication of all specimens:

1 Gusset plates were welded to the end plates by fillet welds using E7018 electrode rods . Welding was done by an experienced welder under careful supervision to ensure adequate penetration. During welding, the end plates were positioned horizontally and the gusset plate vertically, as they would be in real structures.

2 The end and gusset plate assemblies were placed in an assembly jig, shown in Figure 2.11, with the same diagonal dimension as the test frame. Then the angles or channels were cut to size and put in place for welding to gusset plates.

3 At predesignated locations along the specimen, a number of strain gages were installed.

4 Finally, after exercising the frame for a few hours, the specimen was taken out of the jig and placed in the testing frame, as shown in Figure 2.12. Ten to twelve 1-1/4 inch high strength bolts were used to connect the end plates to the test frame.

2.6 Deformation History

2.6.1 Double Angle specimens

A typical deformation history of the double angle specimens is shown in Figure 2.13. The following points were considered in the selection of this deformation history :

1 Deformation sequence should simulate the effect of severe cyclic loading such as the one expected in severe earthquakes. A previous analytical study [8] shows that under severe earthquakes, a braced frames may have story drifts more than 2% of the story height. The 2% drift would result in 2.0 inches of axial deformation in the test specimens. Using A36 grade steel for the test specimens, which usually exhibits yield strength around 45 ksi, the axial deformation is equal to approximately 10 Δ_y, where Δ_y is the axial yielding deformation of the specimen based on F_y=45 ksi.

2 For three reasons, cyclic loading starts with applying tension force: first, to reduce the initial crookedness of the specimen; second, to check the actual yield strength of the specimen as indicated from the flatness of the hysteresis curve, before any buckling occurs; third, to cross-check the load cell calibration factor by using strain gage values in the virgin state in which no residual plastic strain is introduced to the specimen.

3 For the sake of comparison, the deformation history was kept similar to the one used in previous studies [2] and [5].

The length of the specimen increases through cycles. The increase is due to the introduction of plastic deformation into the specimen in the post-buckling region. This increase in axial length, called the "column growth phenomenon", causes a kink (initial curvature) at the level of zero axial deformation. The presence of this kink causes larger level of lateral deformation for the same level of axial deformation, compared to the case for the virgin specimen having no kink. Obviously, the test set-up has a limitation for the maximum level of lateral deformation. Therefore, in their last cycles, some specimens underwent extreme axial compression deformation of slightly less than 10Δy.

2.6.2 Double Channel Specimens

A typical deformation history of double channel specimens, shown in Figure 2.14, simulates severe load reversal that a bracing member may experience in a strong earthquake. For the sake of comparison, the deformation history was kept identical to the one used in the previous study at the University of Michigan.

3 EXPERIMENTAL RESULTS

3.1 Double Angle Specimens

The two sets of specimens consisting of 2L3.5x2.5x1/4 with b/t ratio of 10, and 2L3.5x2.5x3/8 with b/t of 6.7 were investigated. Two different stitch spacings were used for the first set and three different stitch spacings were investigated for the second set. The results are discussed in the following sections .

3.1.1 General Cyclic Behavior

The cyclic deformation histories of double angle specimens are shown in Figure 3.1 through 3.5. The major aspects of the behavior of the specimens are cited in the figures and also tabulated in Table 3.1. All specimens were initially pulled up to an axial tension deformation equal to Δ_y, which generally induced a load less than P_y in the specimens due to their initial crookedness. However, in the subsequent cycles the specimens were pulled up to their yield point indicated from the flatness of the hysteresis loops.

In the gusset plates generally no phenomenon detrimental to specimen performance was observed, since they were designed according to the recommendation of Reference 2. However, an exception was specimen A3 in which, unintentionally, the free length beyond the angle was slightly less than its recommended value, two times the thickness of the gusset plate. Consequently, a small crack developed in the lower gusset plate but it was not very significant. All specimens buckled out of plane, as they were designed for. In all specimens failure mode was associated with fracture in the outstanding compression leg at the location of local buckling. This suggests that any attempt to increase the ductility and energy dissipation capacity of the specimens should be tied to prevention of local buckling or reducing its severity.

A significant drop in the buckling load from the first to the second cycle occurred in all specimens. This is attributed to the geometry effect coming from large slenderness ratio. The buckling load continued to decrease during the later cycles but at a much smaller rate as also indicated by the hysteresis loops of specimens A4 and A5 in Figure 3.6.

The following sections discuss different aspects of the general behavior of all five double angle specimens.

3.1.1.1 Specimen A1

In the first specimen, A1, the stitch spacing was based on AISC Specification requirement, Section 1.18.2.4. The requirement states that "Compression members composed of two or more rolled shapes separated from one another by intermittent fillers shall be connected to one another at these fillers at intervals such that the slenderness ratio l/r of either shape, between the fasteners, does not exceed the governing slenderness ratio of the built-up member". This consideration served its intended purpose, so that no individual angle buckling was observed before the overall buckling of the specimen. It was observed that due to some imperfection and accidental eccentricity overall buckling did not occur when the specimen was perfectly straight. On the contrary, some nonlinearity occurred before overall buckling and consequently at the time of overall buckling the specimen had some curvature even in the first cycle. This curvature increased during subsequent cycles due to residual deformation from previous post-buckling range.

After overall buckling in the so-called "post-buckling range" the specimen underwent bending in its plane of symmetry due to moment applied by P-Δ effect. Immediately after overall buckling, at a point 12" distant from the stitch at mid span in the **lower portion**, the gap between the two angles closed very rapidly and initiation of a plastic hinge was observed at this point. However, the location of the gap closing and plastic hinge shifted to a point symmetrical to the original one i.e., 12" distant from mid span in the **upper portion**, most probably due to strain hardening. The gap closing can be attributed to individual bending of the angles because a sufficient number of stitches were not provided to cause overall bending behavior rather than individual bending behavior. The specimen suffered failure in the welds of the base plate to the gusset plate during cycle 18.

3.1.1.2 Specimen A2

The stitch spacing for this specimen was selected based on the observation of the distance between mid span and the gap closing location in specimen A1. The first cycle pre-buckling behavior was similar to specimen A1. However, due to malfunction of the actuator, the first cycle buckling load was not recorded. In post-buckling range, no gap closing was observed until cycle 5. Thus the specimen exhibited a compound-section behavior rather than individual bending of the two angle components. Gap closing occurred in cycle 5 in which the specimen underwent an axial

compression deformation equal to 3 Δy while for specimen A1 this happened in cycle 1 in which the axial compression deformation was only Δy.

It should also be noted that although the gap closing started at cycle 5 in specimen A2 its complete closing did not occur until cycle 7, in which the extreme axial compression deformation was equal to 5Δy. This shows that closer stitch spacing not only delayed the starting of the gap closing phenomenon to a much larger axial deformation level but also delayed its complete closing for two cycles. The advantages and disadvantages of this delay in terms of buckling load and energy dissipation will be discussed later.

3.1.1.3 Specimen A3

This specimen was one of the three specimens selected to have b/t ratio of 6.7 to comply with Section 2.7 of AISC Specification [14]. This selection was part of an attempt to examine the effect of b/t ratio on member performance. The stitch spacing was selected based on a hypothesis which considers selection of unstitched length in such a way that plastic hinges in individual angles do not occur before the formation of overall plastic hinges in the combined section. So far, in its original form, this hypothesis has not been proven. Nevertheless, this 37" spacing was less than half of the maximum spacing allowed by AISC and yet not enough to prevent the gap closing (individual angle bending) which occurred in cycle 4.

3.1.1.4 Specimen A4

The stitch spacing for this specimen was selected based on an equation in the AISC LRFD Manual [11] indicating lateral support requirement for excessive rotation in beams. Although this requirement is not meant for the case under consideration, it was thought that since the present problem in the post-buckling range involves excessive rotation of the individual angles, this formula may be applicable to prevent gap closing at least at low levels of lateral deformation. The gap closing took place in cycle 4 like in specimen A3 but it had slightly better performance in terms of cyclic buckling load and energy dissipation which will be discussed in later sections.

3.1.1.5 Specimen A5

Since it was observed that the performance of specimen A4 was better than the performance of specimen A3, it was decided to further reduce the stitch spacing from 17" in specimen

A4 to 12" in specimen A5. As mentioned before, this 12" spacing was based on observation in specimen A1 in which 12" distance was measured between the mid span stitch and the gap closing location. Except for the first cycle buckling load, which was the same, the performance of this specimen was inferior to that of specimen A4. Due to limited data at this stage, this difference cannot be explained. More data is needed in order to establish a rational criteria for optimum stitch spacing.

3.1.2 The Mechanism of Gap Closing

In order to understand the mechanism of gap closing, the phenomenon was closely observed in specimen A2. At the onset of the gap closing, the axial deformation was increased at a constant low rate. It was observed that sudden gap closing, which can be an indication of buckling of the individual compression component, did not occur. Instead, gradual gap closing occurred which was an indication of individual bending behavior. One other important point observed in this specimen was that while the gap was completely closed at the bottom of the back-to-back leg, it was to some extent open at the top of this leg, as shown in Figure 3.7.a. This indicated that individual bending occurred about the weak axis of the angle components, z-z, rather than y-y axis. This leads to early closing of the gap at the bottom of the back-to-back legs. This process is schematically shown in Figure 3.7.b. **After close examination of gap closing in specimen A2, it was concluded that this phenomenon involves individual bending of the angle components**. Further understanding of the mechanism of gap closing requires paying attention to the axial load path from the gusset plate to the member near mid span as will be explained in the following paragraph.

The specimen due to overall P-Δ effect experiences a moment that imposes same-direction bending on both angles. This bending causes the specimen to respond as a compound section resulting in an overall curvature in the specimen as shown in Figure 3.8.a. On the other hand, at the end of the specimen, axial load P is partitioned and transferred from the gusset plate to the individual components along the angles' edges. The next stitch is not close enough for these two partitioned axial forces to merge together such that the combined load acts on the overall centroid. Instead, each partitioned axial force acts along the edge of the corresponding angle as shown in Figure 3.8.b. In a free body diagram, transfer of each partitioned axial force to the centroid of the corresponding angle applies bending moment to the two components **in two opposite directions**. These two opposite bending moments make them get closer and reduce the gap in between. It was observed that the rate of

deformation due to this local bending was faster in the component which was under compression, compared to the deformation rate of the tension component. This is attributed to the fact that some part of the compression component had been plastified resulting in a lower modulus of elasticity and consequently a lower bending stiffness. This lower bending stiffness causes faster deformation rate in the compression component. Disadvantages of the gap closing were explained in Section 1.1 and will be further analyzed in the subsequent sections.

3.1.3 Critical Buckling Loads

The measured buckling loads of all specimens during the first ten cycles are given in Table 3.2 and were normalized with respect to their own actual tension yield capacity, P_y.

3.1.3.1 The First Cycle Buckling Load

The measured first cycle buckling loads of all specimens are shown in Table 3.2. The slenderness ratios were calculated based on Ky=1.0. Column 4 specifies the calculated values of the first cycle buckling load from AISC Formula (1.5-2) without using the factor of safety. Tension yield capacities, Py, inserted in Column 3 were determined from the flatness of the hysteresis loop near tension yielding. The measured first cycle buckling load of specimen A1 was 10% more than the calculated one. This difference was 34% and 31% for specimens A4 and A5, respectively. As stated before, the first cycle buckling loads of specimen A2 and A3 were not recorded due to an accident. However, by comparison of the first cycle buckling load of specimen A4 and A5, it can be said that the first cycle buckling load is not a function of the stitch spacing. Higher measured buckling loads compared to the calculated ones can be attributed to the fact that assumption of hinged-end connection may not be perfectly correct. This happens because of some stiffness provided by the gusset plates against out-of-plane rotation which leads to reduction in effective length factor, Ky, which was considered to be equal to 1.0 in the calculation of P_{cr} from AISC formula.

In specimen A1, immediately after the first cycle overall buckling, the gap between the two components was completely closed. This closing occurred due to excessive unstitched length in the specimen while it was not the case for all other specimens which had at least twice the stitches required by the current AISC Specification requires.

3.1.3.2 Cyclic Buckling Loads

Numerical values of cyclic buckling loads of specimen A1 and A2 in Table 3.2 are

presented graphically in Figure 3.9. This figure shows the increasing effect of closer stitch spacing on the cyclic buckling loads, i.e., specimen A2 with closer stitch spacing had consistently higher cyclic buckling load except in cycle 10 in which it failed. Another comparison of cyclic buckling loads is made for the second set of specimens in Figure 3.10. Comparison of specimen A3 with A4 and A5 leads to the same conclusion that cyclic buckling loads for the closely stiched specimens, A4 and A5, were higher than those of specimen A3. However, with regard to cyclic buckling loads, the performance of specimen A5 with a closer stitch spacing of 12" was inferior to that of the specimen A4 with 17" stitch spacing. This cannot be explained at this point due to lack of enough data. Lower cyclic buckling load generally means less energy dissipation in the corresponding cycle which will be shown in a later section.

The cyclic buckling loads of specimen A2 and A5, having the same stitch spacing but b/t ratios of 10 and 6.7, respectively, are compared in order to examine the effect of b/t ratio. Since the slenderness ratios of these specimens were different, cyclic buckling loads were normalized with respect to their own calculated first cycle buckling load. These normalized cyclic buckling loads are indication of the stability of specimen's hysteresis loops. This comparison is presented in Figure 3.11 and the only conclusion from this figure is that during the first two cycles the specimen with smaller width-thickness ratio had higher buckling load while the opposite is true for the rest of the cycles. Due to insufficient data for different b/t ratio, this conclusion also cannot be rationalized.

3.1.4 Local buckling

Failure of all specimens was associated with fracture in the outstanding leg of the angle which underwent compression during post-buckling bending. This fracture is a direct result of severe local buckling while no other major failure was observed. The first two specimens had a b/t ratio equal to 10 complying with Part 1 of AISC Specification. One obvious correlation between local buckling and the stitch spacing can be noticed. Local buckling in specimen A1 started in cycle 3 while in specimen A2 it was delayed to cycle 5. This shows that closer stitch spacing in the first set of specimens delayed the occurrence of local buckling. However, such a correlation was not so obvious in the second set of specimens, A3, A4, A5, for two reasons. First, the second set had a smaller b/t ratio in compliance with Part 2 of AISC Specification. Second, the difference in the stitch spacing was not as drastic as the one in specimens A1 and A2. Consequently, regardless of the stitch spacing,

local buckling occurred around Cycle 6 with extreme compression deformation equal to 3Δy. This may be attributed to the fact that the second set of specimens did not have stitch spacing close to AISC requirement, which for this set of specimens was calculated to be equal to 63". Instead, due to observations in specimens A1 and A2, the stitch spacings were selected as 37, 17, 12 inches for specimen A3, A4, and A5, respectively. By drawing an analogy with the first set of specimens, it may be said that if these specimens had stitch spacing equal to 63", local buckling could have occurred much sooner than cycle 6-- which was the case for specimen A1 with the stitch spacing equal to 71".

In the closely-stitched specimens, the gap closing was a gradual process as the axial deformation increased. However, one common effect of local buckling on the gradual gap closing was to expedite the process. In other words, the gap closing occurred at a much faster rate since local buckling caused the resisting angle section to transform to a mere plate- the back-to-back leg bending out of plane with a very small stiffness. In fact, after local buckling, the gap closing was uniform along the width of the back-to-back leg and the phenomenon explained in Section 3.1.2 and shown in Figure 3.7.b could not be seen thereafter.

3.1.5 Energy Dissipation

An important response parameter for inelastic cyclic loading is the energy dissipated by the bracing member. The energy dissipated during each loading cycle was calculated for all five specimens from their axial load vs. axial displacement plots and it was normalized for the sake of comparison. Normalization is carried out by dividing the amount of dissipated energy by the cross section area of the corresponding specimen. Table 3.3 shows the numerical results for the first ten cycles of all specimens along with the total energy dissipated by each one. The difference in total energy dissipated by 5 specimens cannot be analyzed at this point. Figure 3.12 shows a comparison of the energy dissipation of specimens A1 and A2.

It can be concluded that the cyclic energy dissipation is not a function of the stitch spacing in the first set of specimens with width-thickness ratio of 10. This may stem from the fact that local buckling due to large b/t ratio was so dominant that closer stitch spacing did not affect cyclic energy dissipation capacity. However, the closer stitch spacing could play its role in the second set of specimens in which the local buckling was not a dominant factor due to smaller width-thickness ratio of 6.7. Consequently, closer stitch spacing in the second set of specimens caused more energy to be

dissipated. Figure 3.13 shows that specimens A4 and A5 with smaller stitch spacing dissipated more energy in comparison with specimen A3. Note that energy dissipation in the beginning cycles cannot be a criterion since extreme compression deformation in these cycles was less than $2\Delta y$ and also the calculation of energy dissipation is very sensitive to whether or not predetermined level of extreme compression deformation could be reached. As stated earlier, equal or somewhat inferior performance of specimen A5, with smaller stitch spacing, compared to the behavior of specimen A4 cannot be analyzed at this point.

One final comparison is made between the energy dissipation capacity of specimens A2 and A5 in order to examine the effect of b/t ratio. Figure 3.14 shows that more energy is dissipated by specimen A5 which had a b/t ratio of 6.7 as opposed to 10 for specimen A2. This significant difference is due to the reduction in the severity of local buckling in specimen A2 and is a direct favorable result of smaller b/t ratio.

3.2 Double Channel Specimens

Three different stitch spacings were used for three double channel specimens; the spacing according to current AISC Specifications, the continuous stitch, and the spacing twice closer than what the current AISC Specifications [14] requires. The results are discussed in the following sections.

3.2.1 General Cyclic Behavior

The cyclic deformation histories of double channel specimens are shown in Figure 2.14. Like double angle specimens, all specimens were initially pulled up to an axial tension deformation equal to Δ_y which generally induced a load less than P_y in the specimens due to their initial crookedness. The initial crookedness was reduced or completely eliminated due to this sequence of axial deformation. All specimens were subjected to cyclic loading until fracture developed through more than half of the section. All specimens buckled in the plane of the test frame which was perpendicular to the channel web.

The following sections discuss different aspects of the general behavior of all three double channel specimens.

3.2.1.1. Specimen C1

Specimen C1 was made of 2C5x6.7 American standard channels with an effective

slenderness ratio of 50. The specimen had a clear stitch spacing of 21" while the minimum requirement is 24" according to current AISC specifications [14]. In the first cycle prior to reaching the buckling load, the specimen started to bend considerably in a sine-shaped configuration. Further bending caused formation of three plastic hinges: one at mid span and two others at the end points close to the gusset plates. Further increase of axial deformation caused the mid span plastic hinge to suddenly shift to a point very close to the first stitch at the upper end. This shifting of mid span plastic hinge caused the formation of a unique triangular buckling shape as shown in Figures 3.15.a and 3.15.b. At this stage, local buckling occurred at the location of the plastic hinge in both the flanges and the webs of the channels. In the subsequent cycles, the severity of local buckling increased rapidly due to excessive hinge rotation and consequently the compressive strength of the member deteriorated. At the end of the first cycle, cracking initiated in the flange next to the location of plastic hinge and developed throughout the whole section in the subsequent cycles. This specimen lasted only three cycles and it was subjected only to a maximum axial compressive deformation of $5\Delta_y$. Figure 3.16 shows the fracture in the specimen C1 at location next to the first stitch.

3.2.1.2 Specimen C2

Specimen C2 was made of 2C4x5.4 American standard channels with an effective slenderness ratio of 56. The two channels were connected to each other by continuous weld which makes them like a rectangular tube section. In the post-buckling range, a sine-shaped configuration was formed with one plastic hinge at mid span and two others at the ends, as shown in Figure 3.17. A minor local buckling occurred at mid span in Cycle 3 but its growth was slow until cycle 11. In cycle 12 in which the maximum compressive deformation was increased to $15\ \Delta_y$, the local buckling became more severe and two more plastic hinges formed at the two ends of the member next to the gusset plates. Increase in the severity of local buckling caused the cross section to distort as shown in Figure 3.18. The distortion caused the webs of the channels to reduce the space in between whereas it caused the toes of the channels to get farther out. Consequently, fracture was initiated near mid span in the weld connecting toes of the channels and the moment capacity of the member dropped drastically. This drop caused more pinching of the hysteresis loops. This specimen lasted 20 cycles and it survived several cycles of maximum axial compressive deformation of $15\Delta_y$.

3.2.1.3 Specimen C3

Specimen C3 was made of 2C4x5.4 American standard channels with an effective slenderness ratio of 56. Based on the observation of the test of Specimens C1 and C2, it seems that the current method of nominal design for stitches is inadequate to provide the strength required in the post-buckling range. The poor performance of Specimen C1 as opposed to the good energy dissipation of Specimen C2 suggested the use of a closer stitch spacing for Specimen C3. A stitch spacing of 10" was used in Specimen C3 which is approximately half of the maximum stitch spacing allowed by AISC Specification [14]. The behavior of this specimen was very similar to the behavior of Specimen C2. One plastic hinge formed within the unstitched length, some distance from the mid span stitch. The mid span plastic hinge did not form exactly at the stitched portion indicating that the plastic modulus was slightly higher than the plastic modulus of the unstitched portion. The two other plastic hinges formed at the ends next to the gusset plate as shown in Figure 3.19. A minor local buckling occurred in the concave-side component at the location of the lower plastic hinge. A fracture initiated in the weld of the mid span stitch in cycle 9 which was followed by a complete tearing of the weld in cycle 15. The specimen lasted 24 cycles in which a complete fracture was developed in the concave-side channel.

3.2.2 The Effects of Stitch Spacing

The effects of the stitch spacing on the performance of the three double channel specimens are discussed in the following sections. The performance is discussed with regard to post-buckling shape, the distortion of the section, the fracture life, and the energy dissipation capacity.

3.2.2.1 Post-Buckling Shape

Buckling shapes of the tested specimens were a sine-shaped curve at the start of buckling. This kind of buckling shape was maintained in post-buckling range until the failure in the case of specimens C2 and C3, which had continuous stitching and twice the number of the stitches required by current AISC Specification [14], respectively. As for Specimen C1 with 21" stitch spacing as per current AISC Specification [14], a different post-buckling shape was observed. At the first buckling load, a sine-shaped buckling curve was observed first. As the lateral displacement increased further, the plastic hinge suddenly shifted towards the top, and formed next to the first stitch from the top end, as shown in Figure 3.15.a and 3.15.b. This plastic hinge shift is clearly due to too

large stitch spacing as given by the current design specification.

The mechanism of shifting of the plastic hinge and consequent change of buckling shape is believed to be that when the stitch spacing is larger than a certain value, the two channels are able to bend individually. The moment capacity in that portion of the member is significantly reduced from that of the combined section and the load sustained by the member drops. This results in the change of buckling shape and consequently loss of energy dissipation capacity and early failure. It should be possible to formulate a theoretical model to determine such a critical spacing for a member.

Test results showed effects of different stitch spacing. It affected the rate of the drop in buckling load and the energy absorption capability of the specimens. Figure 3.20 shows the drop in buckling loads with the number of cycles for the three specimens .

3.2.2.2 Distortion of Section

For built-up double channel section the two channels tend to bend individually when stitch spacing is large. This results in distortion of section, as shown in Figure 3.18, and reduction of moment capacity. Stitches play an important role in that they should hold two channels as one single unit. The strains at the edge of channel flanges are thus smaller and distortion of the section would not occur. However, for unstitched portion, single channel behavior takes place and channel flange is then subjected to large strains and section distortion occurs. Test results showed that section distortion was more severe in specimen C1 than in specimen C2 and more severe in specimen C2 than in specimen C3. Stitches are very important in keeping section from distortion and maintain its moment capacity to a certain degree.

3.2.2.3 Fracture Life

The stitch spacing of specimen C1 was designed per current design criteria. It resulted in large distortion of the section, early fracture at the plastic hinge location after only a few cycles, and very fast development of the crack. The reason for that is partly due to larger hinge rotations compared to normal sine-shaped buckling mode under the same axial deformation and partly due to distortion of the sections. Both of these are again attributed to large spacing of the stitches. The life of specimen C1 was much shorter than specimen C2 and specimen C3. specimen C2 and C3 showed greatly improved behavior in terms of ductility and energy dissipation.

3.2.2.4 Energy Dissipation

Energy dissipation per unit area is shown in Table 3.4 for the three specimens. This shows that the closer the stitches, the more energy dissipated . Test result of specimen C1 also implies that bracing members with large stitch spacing can have much shorter life and less energy dissipation.

3.2.3 The Effects of Stitch Strength

For the specimens tested, fractures occurred in several stitches, which indicated that the stitches were subjected to large strains or forces. This resulted in reduction in moment capacity and shorter member life. Nominal stitch strength design does not seem adequate for bracing members subjected to large cyclic deformation in post-buckling range as also observed by previous investigators [1].

4 SUMMARY OF TEST RESULTS

4.1 Double Angle Specimens

Summary of the effect of two parameters in this study i.e., the stitch spacing and width-thickness ratio on the behavior of double angle specimens is presented in this section.

4.1.1 The Effects of Stitch Spacing

Examination of the performance of the two sets of specimens indicates that:

1 Closer stitch spacing causes smaller drop in cyclic buckling loads.

2 Closer stitch spacing delays the gap closing which, due to reduction in the moment capacity, has a pinching effect on the hysteresis loop.

3 Closer stitch spacing delays local buckling since it causes compound section behavior which helps reducing the strain levels.

4 In the case of larger b/t ratio of 10, closer stitch spacing has no effect on the cyclic energy dissipation of the specimens having larger b/t ratio of 10. This is due to the domination of local buckling effect. Closer stitch spacing causes more energy dissipation in the specimens having smaller b/t ratio of 6.7. The difference in total energy dissipation cannot be further analyzed at this point.

4.1.2 The Effects of Width-Thickness Ratio

The following points are indicated by comparison of the behavior of specimens A2 and A5 which had the same stitch spacing, 12", but b/t ratio of 10 and 6.7, respectively:

1 Since failure in all cases was due to fracture at the location of local buckling, as shown in Figure 4.1, any attempt to increase the energy dissipation capacity should be related to the prevention of local buckling or reducing of its severity.

2 Larger b/t ratio causes smaller cyclic energy dissipation which is a direct result of more severe local buckling.

4.2 Double Channel Specimens

4.2.1 The Effects of Stitch Spacing

Test results obtained thus far have shown that some "secondary factors" in member design such as the stitch spacing and the stitch strength turned out to be very important. They can cause severe problems and even result in early failures of members. Stitches were also found to have strong influence on the ductility and energy dissipation capacity of built-up double channel bracing members. From the test results, it is clear that the stitch design is extremely important for built-up double channel sections subjected to large load reversals. Current nominal design criteria for stitches

appear adequate to prevent individual channel buckling before overall buckling of the member. However, they do not ensure the built-up section to behave as a single unit section under reversed loading involving inelastic axial deformation in the post-buckling range. Therefore, modifications are needed in the stitch design requirements. Based on the test results so far, it can be stated that **large stitch spacing** has the following effects:

1 It lowers the compressive load capacity during the post-buckling range in subsequent cycles.

2 It increases the severity of local buckling and the distortion of cross section at plastic hinges.

3 It causes early fracture and member failure.

4 It lowers the amount of energy dissipation.

5 SUGGESTIONS FOR FUTURE INVESTIGATION

5.1 Double Angle Specimens

Due to the observed behavior of conventional (back-to-back) configuration of double angle bracing specimens and also lack of enough information to analyze some of the results of this study, the following suggestions are made for future investigation.

5.1.1 Section Configuration

Failures in all specimens were associated with fracture in the compression leg at the location of local buckling. Thus, it is thought that conventional configuration for double angle bracing members may not be the most efficient one. An alternative configuration which promises a better performance is placing the angles toe to toe. This new configuration, as shown in Figure 5.1.a, is expected to have the following advantages:

Local Buckling : Following favorable conditions will be provided with regard to delaying and reducing the severity of local buckling:

1 Free edge of the angles will be located close to the neutral axis in which the strain levels caused by bending in the post-buckling range is minimum.

2 Stitches will provide support for the free edges against local buckling and prevent deformation of cross section as well.

3 At the location of maximum strains caused by P-Δ effect, the angles will have supported edge (heel) instead of a free edge.

Stiffness : In some cases, moment of inertia of the section in the new configuration can be larger as high as 10%, compared with the moment inertia in the conventional configuration. The larger stiffness causes smaller lateral deflection for the same level of axial deformation. With a smaller lateral deflection, the specimen is able to sustain a larger axial force since multiplication of axial force and lateral deflection is constant and equal to the plastic moment capacity of the section.

Plastic Modulus: For some sections plastic modulus of the section in the new configuration can be up to 20% more than the plastic section modulus of the conventional configuration.

5.1.2 Width-Thickness Ratio

The current upper limit of width-thickness ratio recommended by Part 2 of AISC Specification [14] is based on two studies performed by Gerard and Becker [4] and Haaijer and

Thurlimann [9] in the late 50's. The first one was essentially performed for NACA (National Advisory Committee for Aeronautics) to establish K values for different boundary conditions in plate buckling. The experimental part of the second study was performed on scaled model of plates and angles which did not simulate the post-buckling conditions which are involved in seismic response of bracing members in general and built-up sections in particular. Furthermore, it was performed under monotonic loading and did not include the effect of cyclic loading.

In order to more rigorously examine the effect of the local buckling on the bracing performance under cyclic loading, tests of specimens with different width-thickness ratio should be conducted. The comparison of performance can be made in terms of normalized cyclic buckling loads and energy dissipation per unit area of those members.

5.1.3 Boundary Condition

The hinged-end condition in bracing members causes the members to form two plastic hinges in the two end gusset plates along with one other plastic hinge at mid length of the member. The plastic hinges in the gusset plates do not dissipate significant amount of energy because of low plastic modulus in out-of-plane direction. It is thought that adding stiffening plates normal to gusset plates will significantly increase their out-of-plane plastic modulus such that end plastic hinges will be shifted into the bracing member. This shift of plastic hinges has two favorable effects. First, it reduces the effective slenderness ratio of the member into half, thus, reducing the pinching of the hysteresis loops in the post-buckling range which is characteristic of the members with large slenderness ratio. Second, it leads to a significant increase in the energy dissipation capacity of the bracing member since the member has larger plastic section modulus than the gusset plates. It is suggested that tests be performed on the specimens with the proposed configuration and fixed boundary condition for different b/t ratio. The results of those tests can form the basis for rational design criteria for double angle bracing members with improved ductility and energy dissipation.

5.2 Double Channel Specimens

For double channel specimens more tests are needed in order to develop and verify the theoretical model and suggest new criteria for the stitch design for both spacing and strength. Tests should be performed on specimens with different slenderness ratios in order to develop more general design criteria.

REFERENCES

1 Astaneh-Asl, A., Goel, S.C.," Cyclic In-Plane Buckling of Double-Angle Bracing," Journal of the Structural Division, ASCE, Vol.110, No. 9, September, 1984.

2 Astaneh-Asl, A., Goel, S.C., Hanson, R.D., " Cyclic Out-of-Plane Buckling of Double-Angle Bracing," Journal of the Structural Division, ASCE, Vol.111, No. 5, May, 1985.

3 Ballio, G., Gobbeti, A. and Zanon, P., "Analytical Computations of Dynamic Behavior of Pin Jointed Structures," Proceedings of The First International Conference on Environmental Forces on Engineering Structures, London, July 1979, pp. 459-472.

4 Bekker H. and Gerard G.," Handbook of Structural Stability, Part I - Buckling of Flat Plates," Technical Note 3781, National Advisory Committee for Aeronautics (NACA), Washington D.C., July 1957.

5 Black, R.G., Wenger, W.A., and Popov, E. P., "Inelastic Buckling of Steel Struts Under Cyclic Load Reversals," Report No. UBC/ EERC-80/40, University of California, October, 1980.

6 El-Tayem, A. A., and Goel, S. C.," Cyclic Load Behavior of Angle X-Bracing," Journal of the Structural Division, ASCE, Vol.112, No. 11, May, 1986.

7 Goel S. C., and Xiadong ,T., " Seismic Design of Braced Steel Frames," Proceedings of a Session at Structures Congress 1986 Sponsored by the Structural Division of American Society of Civil Engineers, September 1986, pp. 16-31.

8 Goel, S.C., Hanson, R.D., and Jain, A. K., "Hysteresis Behavior of Bracing Members And Seismic Response of Braced Frames with Different Proportions," Report No. UMEE 78R3 , Department of Civil Engineering , University of Michigan, Ann Arbor, Michigan, July, 1978.

9 Haaijer G. and Thurliman B., "On Inelastic Buckling in Steel," Transactions, ASCE, 125 (1960), pp. 308-344.

10 Hanson, R.D., and Kahn, L.F., "Inelastic Cycles of Axially Loaded Steel Members," Journal of the Structural Division, ASCE, Vol.102, No. ST5 , Proc. Paper 12111, May, 1976.

11 American Institute of Steel Construction, "Load and resistance Factor Design," First Edition, Chicago, Illinois, 1986.

12 Popov, E. P., Takanashi, K., and Roeder, C.W., " Structural Steel Bracing Systems: Behavior Under Cyclic Loading ," Report No. UBC/ EERC-76/17, University of California, October, 1976.

13 Singh, P., "Seismic Behavior of Braced Steel Frames," Report No. UMEE 77R1, Civil Engineering Department , University of Michigan, Ann Arbor, Michigan, July, 1977.

14 American Institute of Steel Construction, "Steel Construction Manual," 8th ed., Chicago, Illinois, 1980.

TABLES

Table 2.1 - Geometric Properties of Double Angle Specimens

1	2	3	4	5	6	7	8
TEST SPEC.	SECTION	A (in^2)	$\frac{K_x L}{r_x}$	$\frac{K_y L}{r_y}$	$\frac{b}{t}$ (1)	$\frac{b}{t}$ (2)	STITCH SPACING (in)
A1	2L 3.5X2.5X1/4	2.88	63	130	10	14	71 (3)
A2							12 (4)
A3	2L 3.5X2.5X3/8	4.22	65	117	6.7	9.3	37 (5)
A4							17 (6)
A5							12 (4)

(1) Outstanding leg.

(2) Back-to-back leg.

(3) Based on $\frac{l_{unstitched}}{r_s} < \left(\frac{K_y L_y}{r_y}\right)_{overall}$.

(4) Based on observation of distance between gap closing location and stitch in previous test.

(5) Based on a hypothetical theory.

(6) Based on LRFD lateral support requirement for exessive rotational capacity $\frac{146\, r_y}{\sqrt{F_Y}}$.

Table 2.2 - Geometric Properties of Double Cannel Specimens

1	2	3	4	5	6	7	8	9	10
SPECIMEN	SECTION	SECTION AREA	kL/r in plane	kL/r out of plane	b/t flange single	b/t flange compound	b/t web	Fy	STITCH SPACING
C1	C5X6.7	1.97	50	35	5.5	9.8	18.4	53	21
C2	C4X5.4	1.59	56	44	5.4	9.5	14.3	46	0
C3	C4X5.4	1.59	56	44	5.4	9.5	14.3	unknown	10

Table 3.1 - Major Aspects of the Behavior of the Double Angle Specimens

SPEC.	$\frac{b}{t}$	STITCH SPACING [IN]		START OF GAP CLOSING	START OF LOCAL BUCKLING
		USED	AISC	CYCLE	CYCLE
A1	10	71	71	1	3
A2		12		5	5
A3	6.7	37	63	4	7
A4		17		4	6
A5		12		4	6

Table 3.2 - Buckling Loads of Double Angle Specimens for the First Ten Cycles

1	2	3	4	5	6	7	8	9	10	11	12	13	14
SPEC.	$\frac{K_yL}{r_y}$ (1)	Py (2) (Measured) kips	$\frac{P_{cr}}{P_y}$ (3) (4) AISC	MEASURED $\frac{P_{cr}}{P_y}$ DURING FIRST TEN CYCLES									
				1	2	3	4	5	6	7	8	9	10
A1	130	135	.361	.398	.240	.202	.181	.178	.155	.156	.145	.145	.120
A2		135		----	.261	.260	.254	.232	.209	.207	.191	.184	.083
A3	117	198	.446	----	.332	.244	.221	.220	.203	.199	.193	.191	.184
A4		198	.446	.597	.397	.329	.286	.257	.236	.226	.216	.205	----
A5		193	.457	.600	.366	.305	.264	.234	.216	.197	.190	.185	.182

(1) Based on Ky=1.0 and L=142".

(2) Measured from hysteresis curve.

(3) Based on Formula (1.5-2) without using factor of safety.

(4) C_c Calculated based on actual Fy and not the nominal one.

Table 3.3 - Energy Dissipation of Double Angle Specimens for the First Ten Cycles

SPEC.	b/t	STITCH SPACING [in]	CYCLE ENERGY DISSIPATION ($\frac{k\text{-}in}{in^2}$)										TOTAL ENERGY DISSIPATED (k-in/in2)
			1	2	3	4	5	6	7	8	9	10	
A1	10	71	6.6	10.2	15.1	14	12.9	16.9	17.7	21.4	26.9	30.1	301
A2		12	----	5.6	10.2	15.1	15.5	16.9	19.1	19	30	35.8	195
A3	6.7	37	----	20	23	21.4	24.8	27.1	28.8	31.6	39.3	42.4	404
A4		17	7.4	20.9	30.6	33.9	37.6	34.9	39.7	42.1	40.4	14.1	301
A5		12	7.4	21.3	25.8	31	38.3	38	34.6	37.3	41.4	46	392

Table 3.4 - Total Energy Dissipation of Double Channel Specimens

SPECIMEN	ENERGY ($k\text{-}in/in^2$)	CYCLES SURVIVED	FRACTURE CYCLE
C1	140 (a)	3	1
C2	731 (b)	20 (C)	13
C3	628 (b)	23	9

(a) Total energy dissipated
(b) Energy dissipated up to Cycle 20
(c) In Cycle 20, the test was stopped.

FIGURES

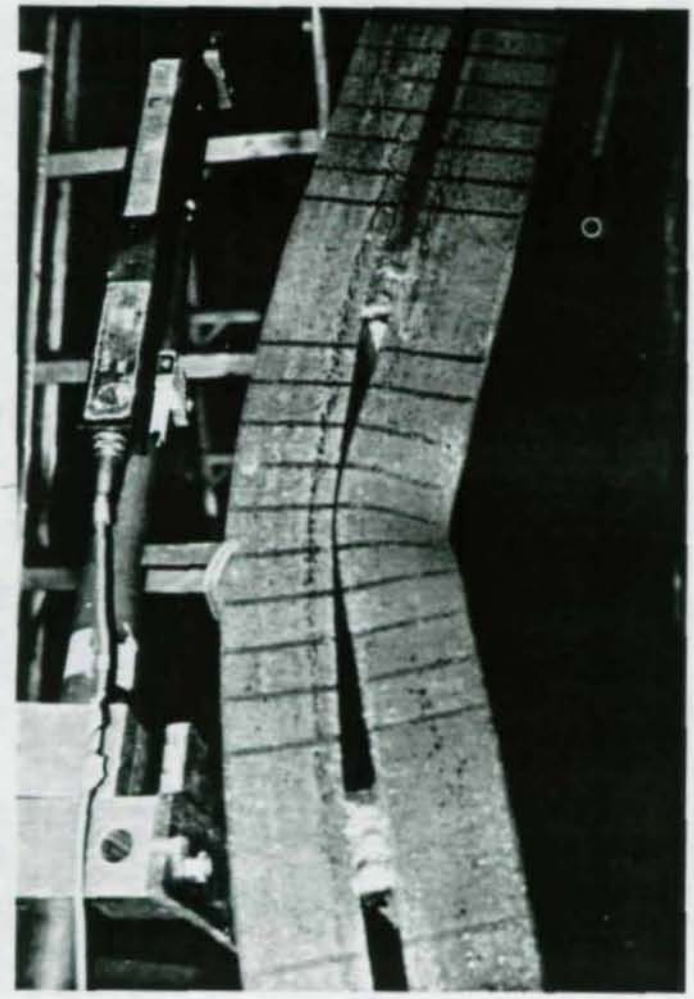

Figure 1.1 - Closing of the Gap in Double Angle Specimen

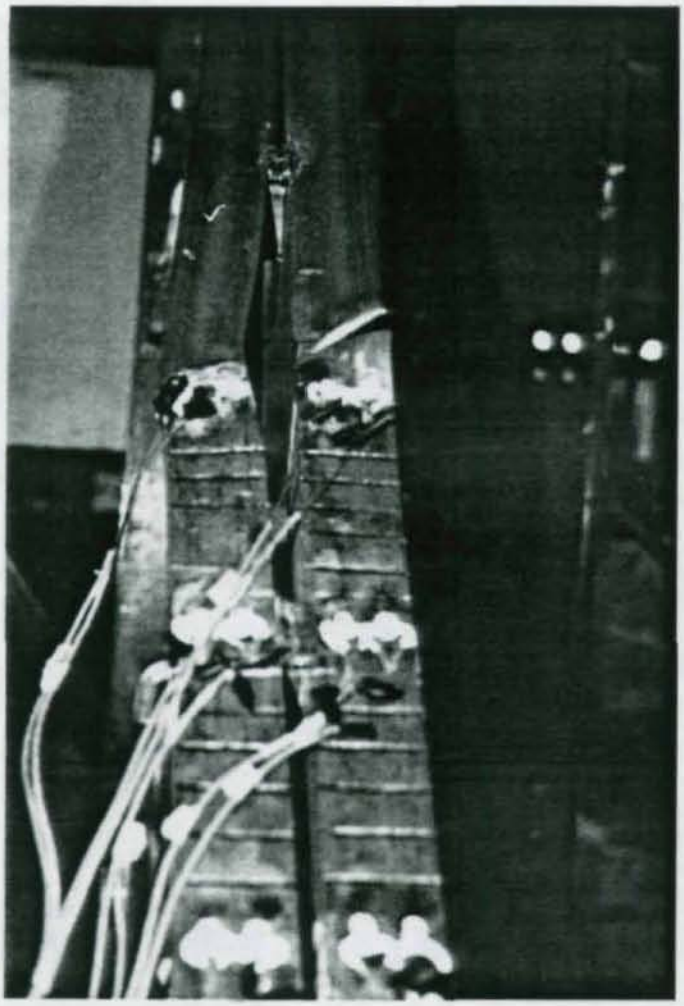

Figure 1.2 - More Curvature in Tension Component Due to Individual Bending in the Post-Buckling Range

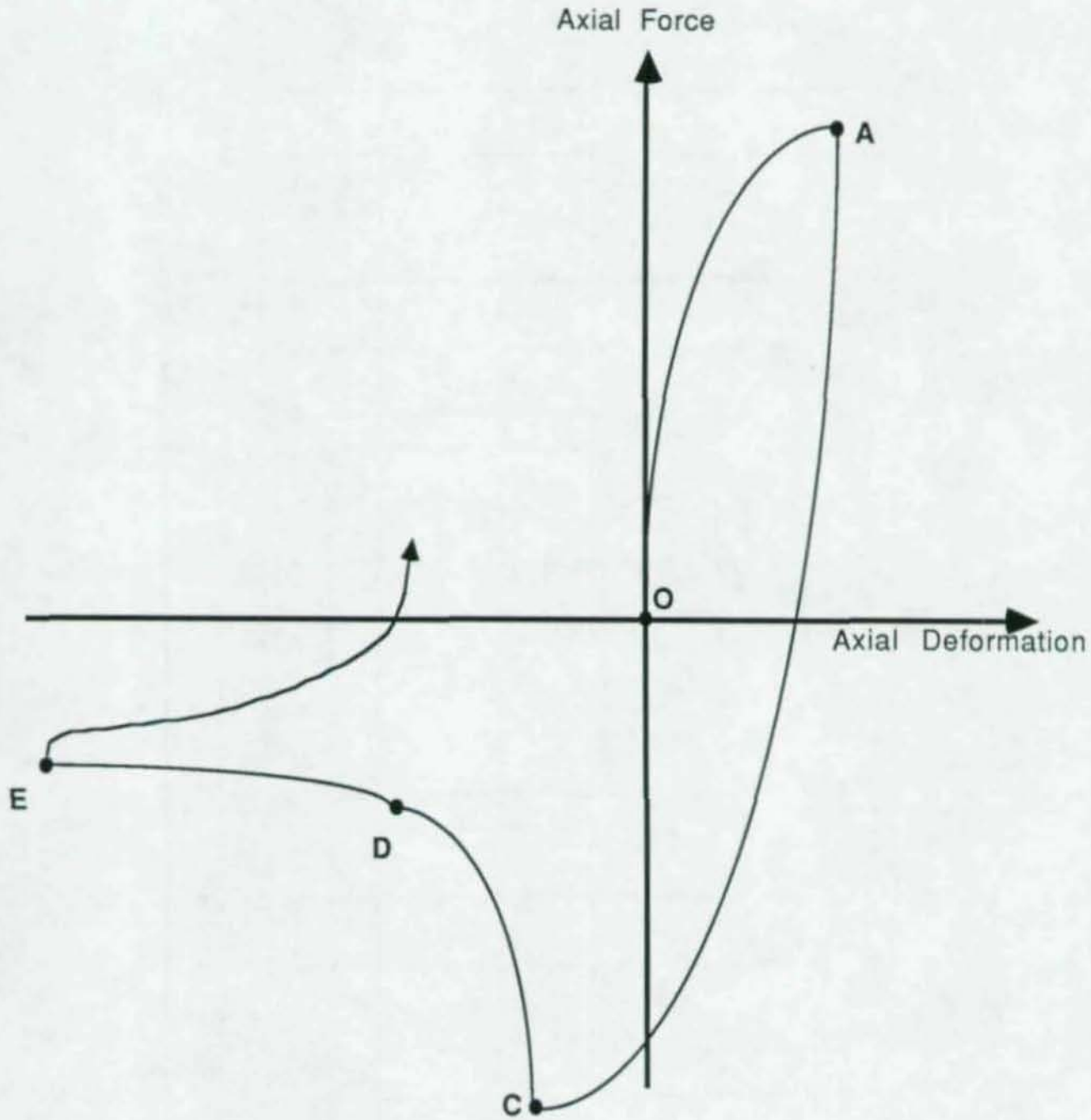

Figure 1.3 - General Hysteresis Loop of Bracing Members

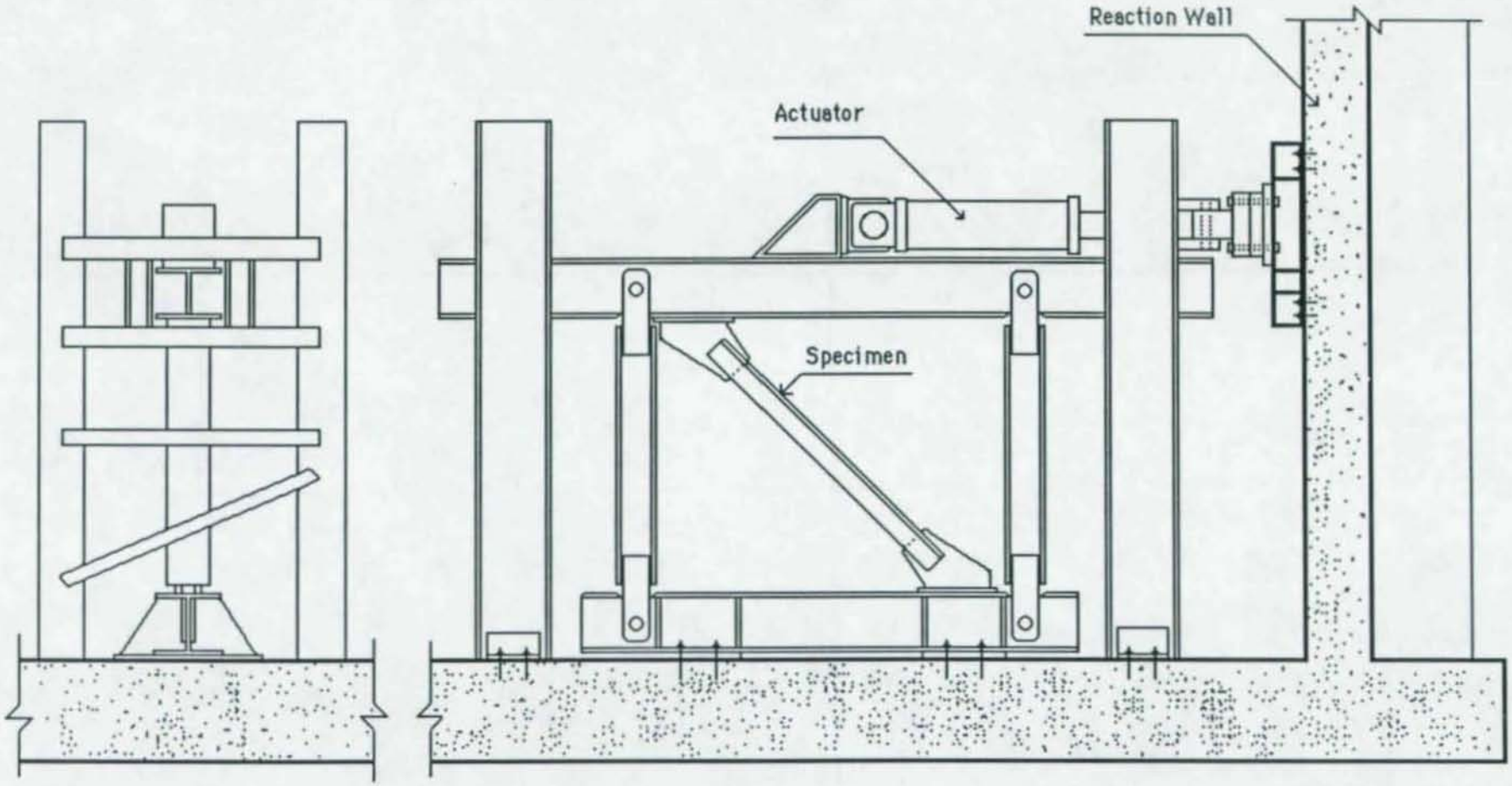

Figure 2.1 - Test Set-Up and Loading System

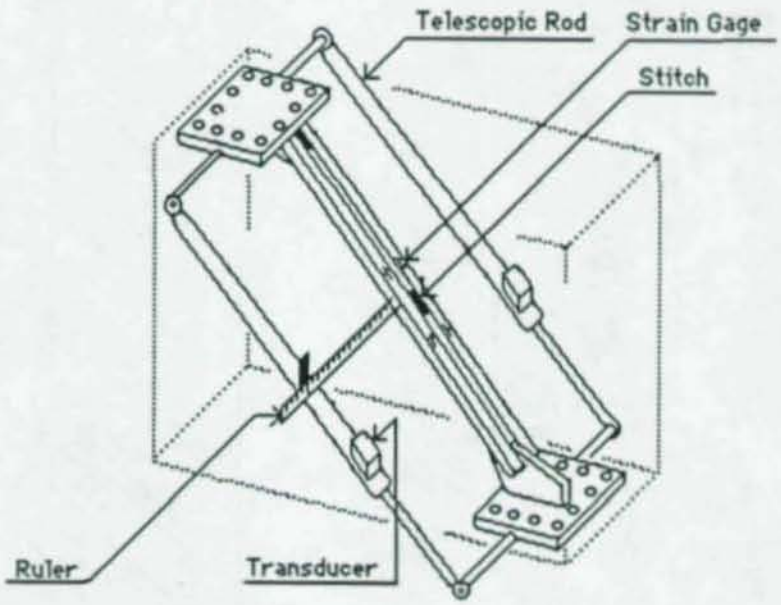

Figure 2.2 - Instrumentation

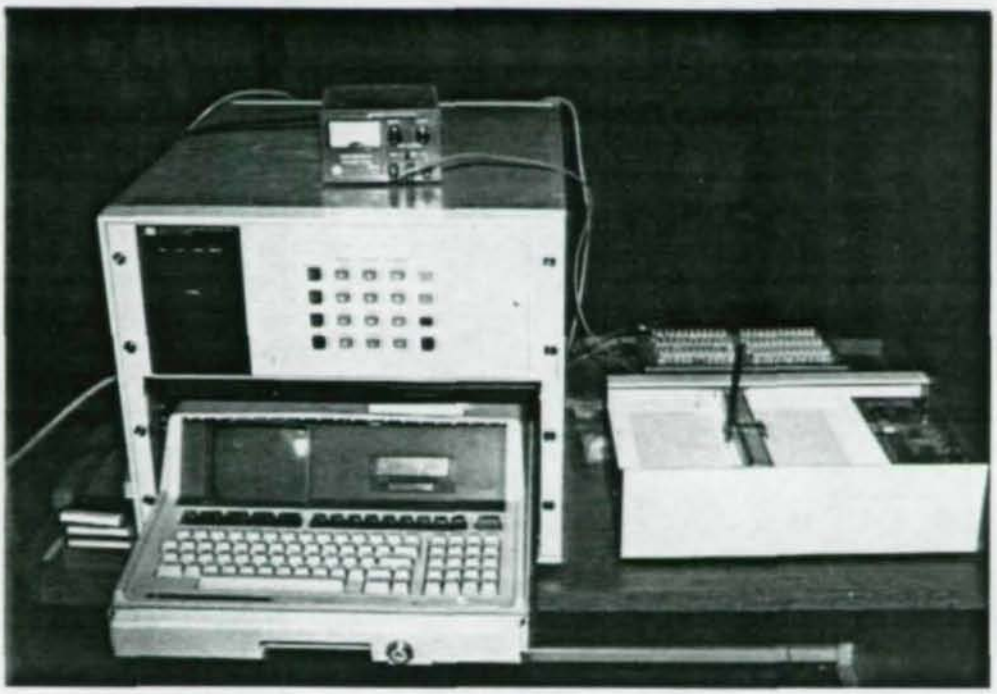

Figure 2.3 - Data Acquisition System

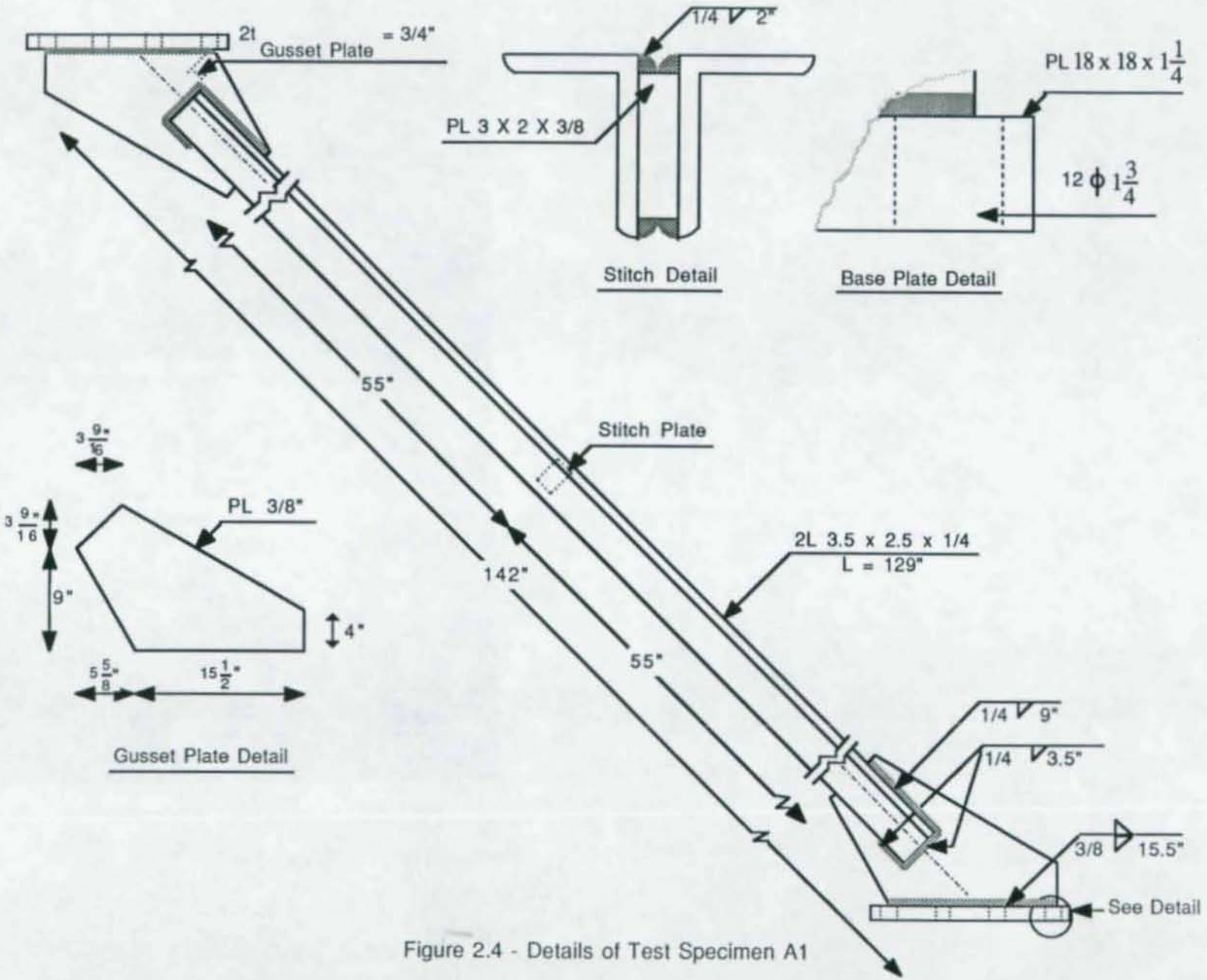

Figure 2.4 - Details of Test Specimen A1

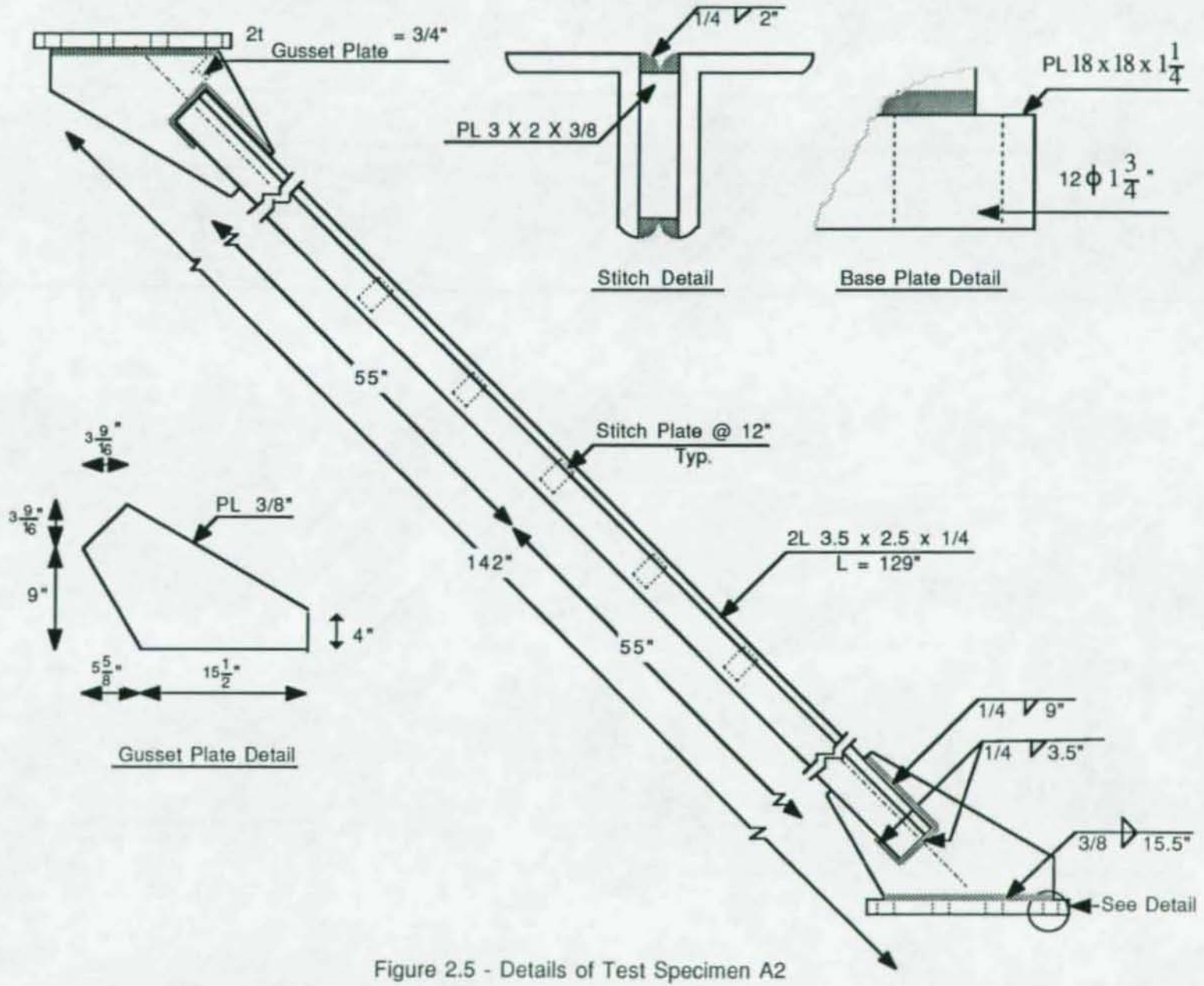

Figure 2.5 - Details of Test Specimen A2

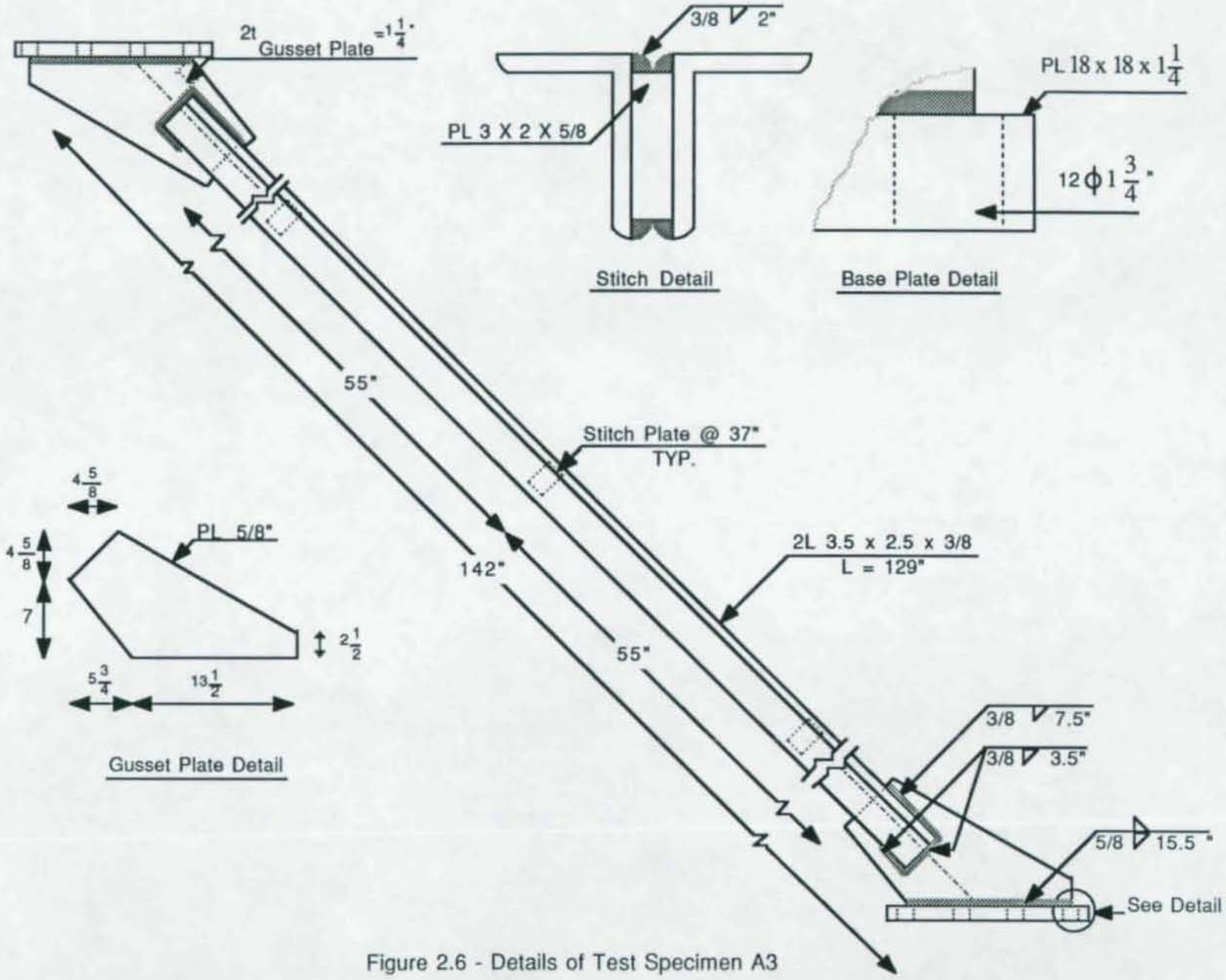

Figure 2.6 - Details of Test Specimen A3

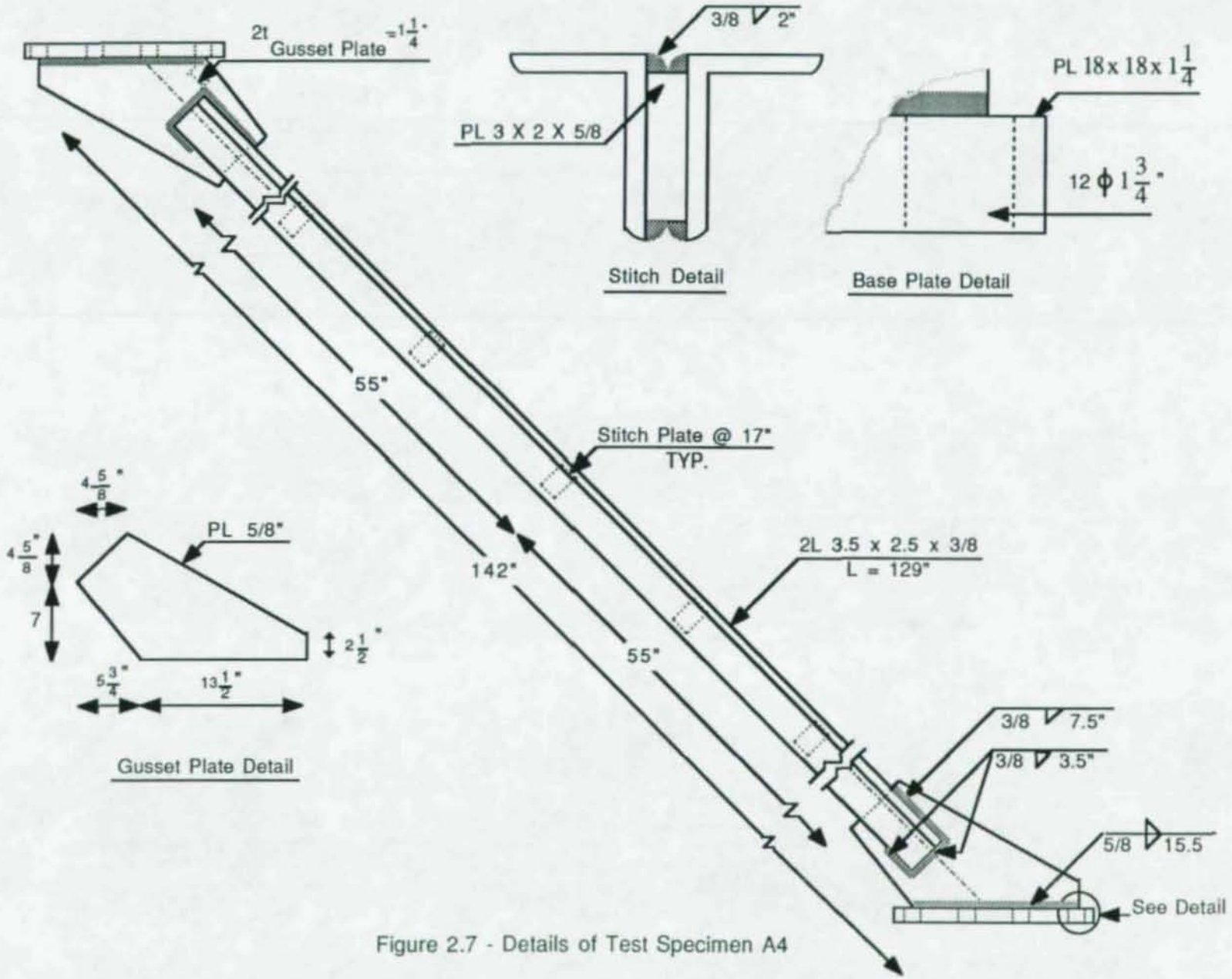

Figure 2.7 - Details of Test Specimen A4

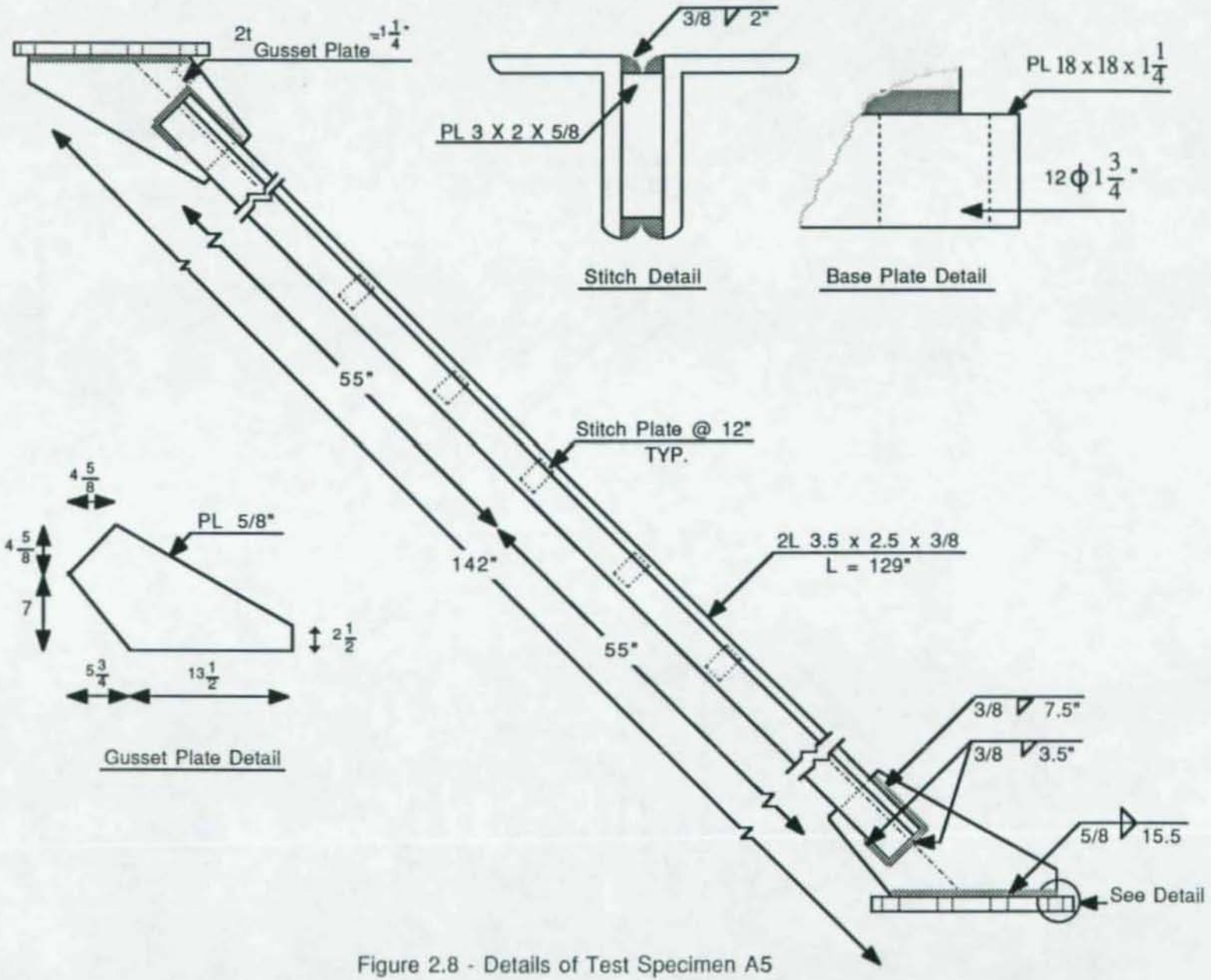

Figure 2.8 - Details of Test Specimen A5

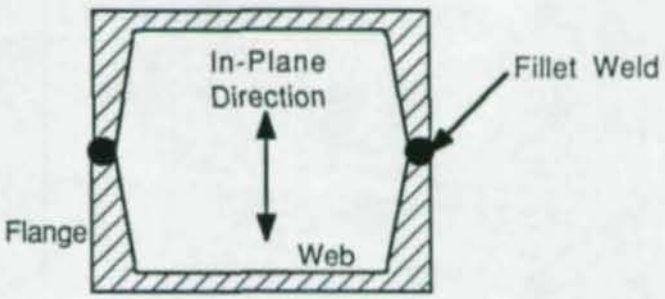

Figure 2.9 - Cross Section of Double Channel Specimens

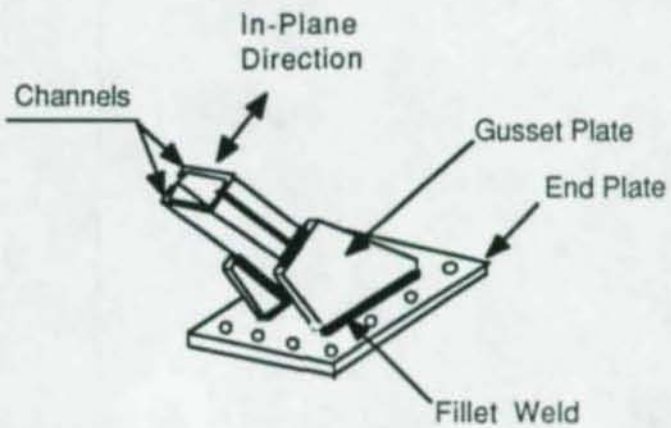

Figure 2.10 - End Connection of Double Channel Specimens

Figure 2.11 - Assembly Jig

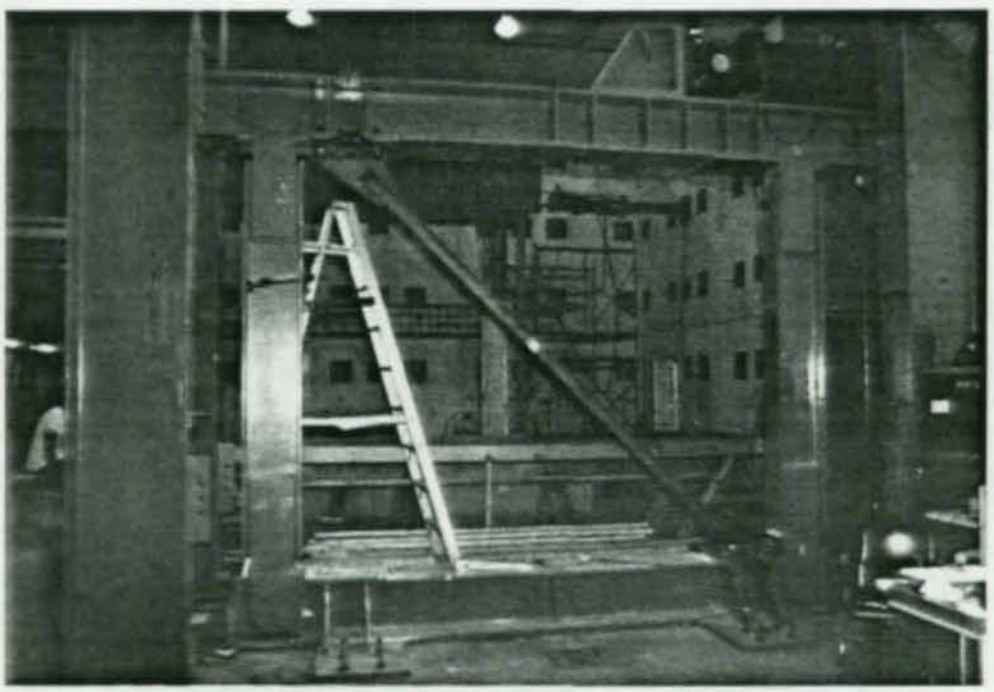

Figure 2.12 - Mounting of a Specimen in the Test Frame

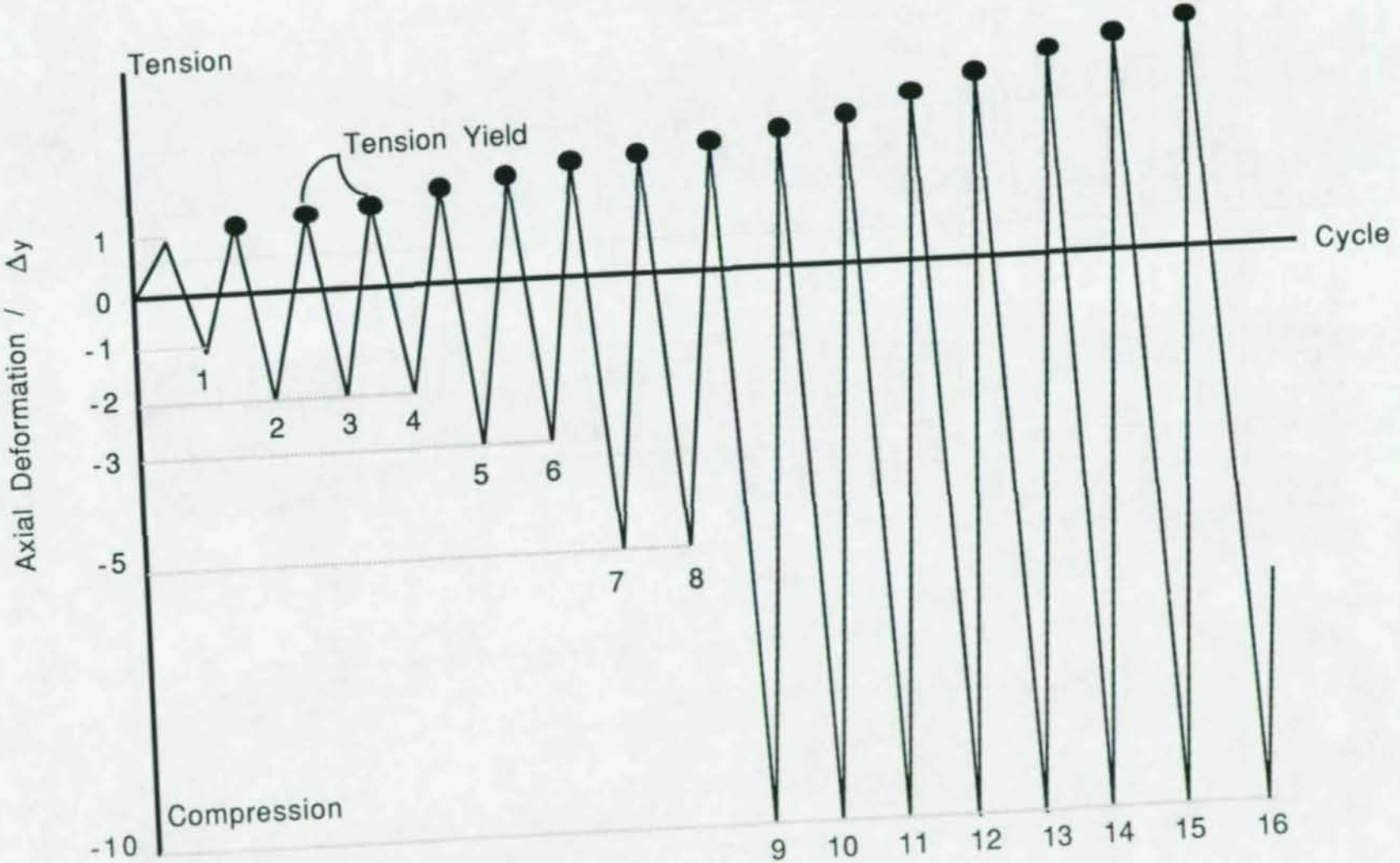

Figure 2.13 - General Loading History of Double Angle Specimens

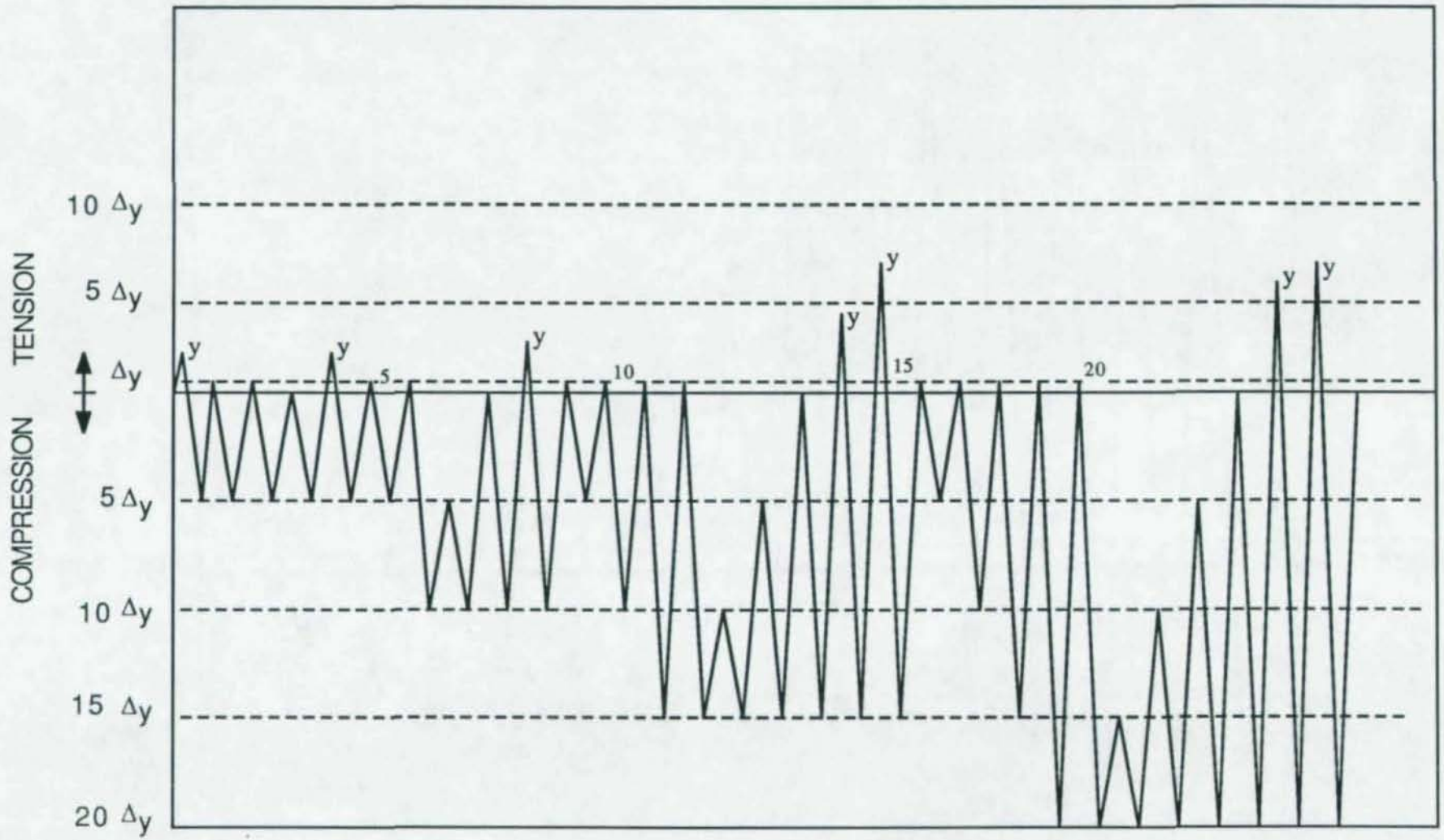

Figure 2.14 - General Deformation History of Double Channel Specimens

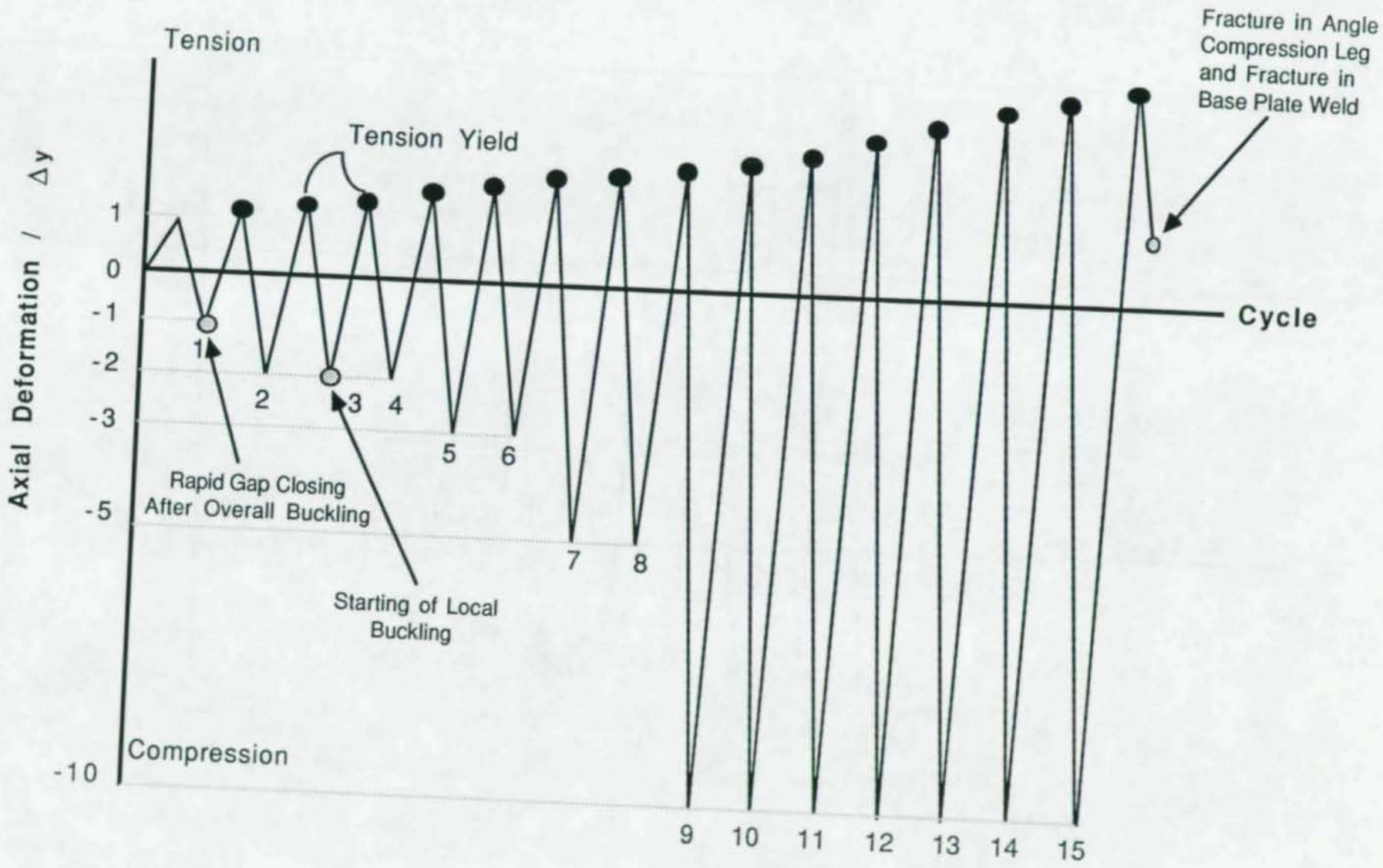

Figure 3.1 - Loading History and Major Aspects of the Behavaior of Specimen A1

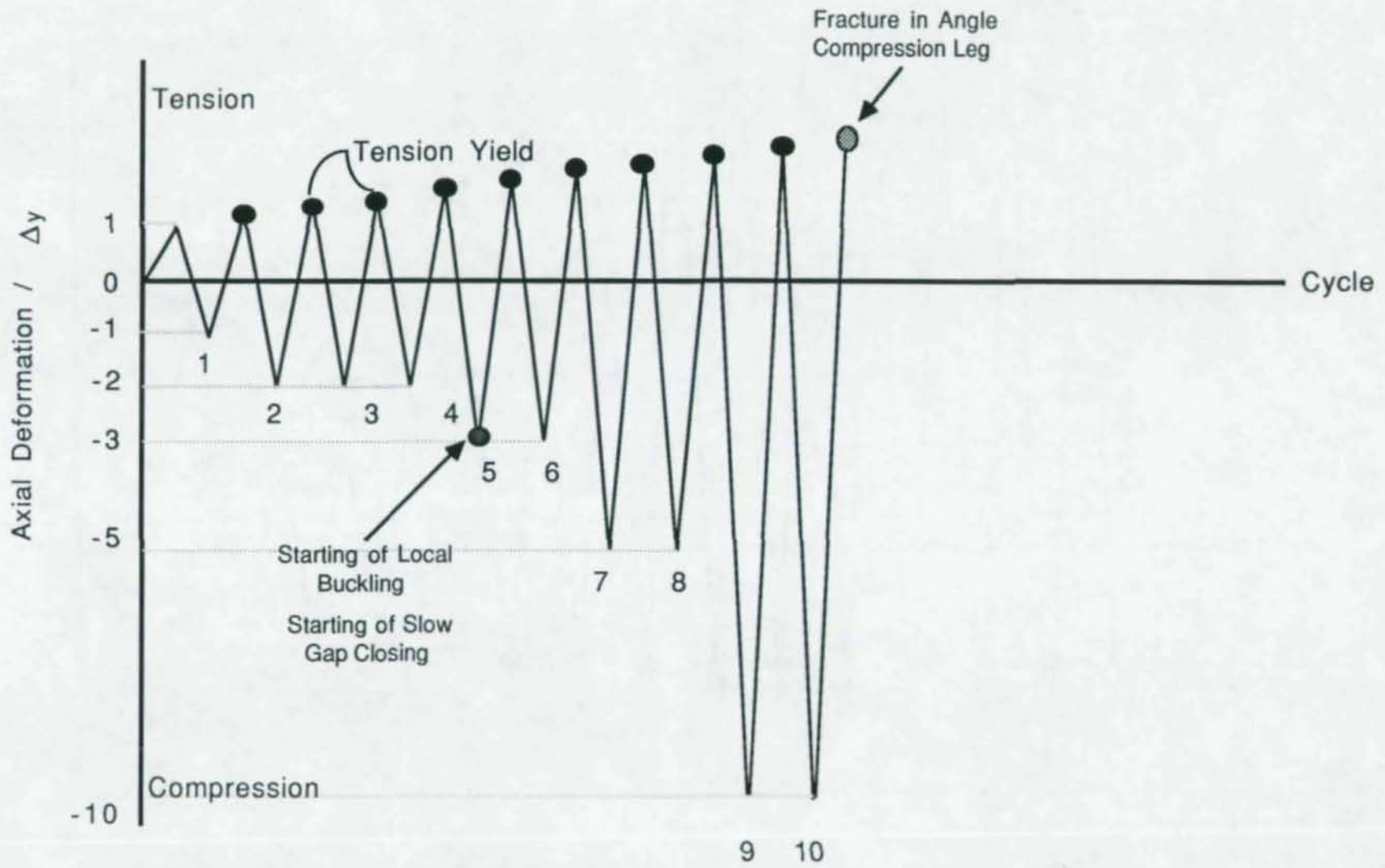

Figure 3.2 - Loading History and Major Aspects of the Behavaior of Specimen A2

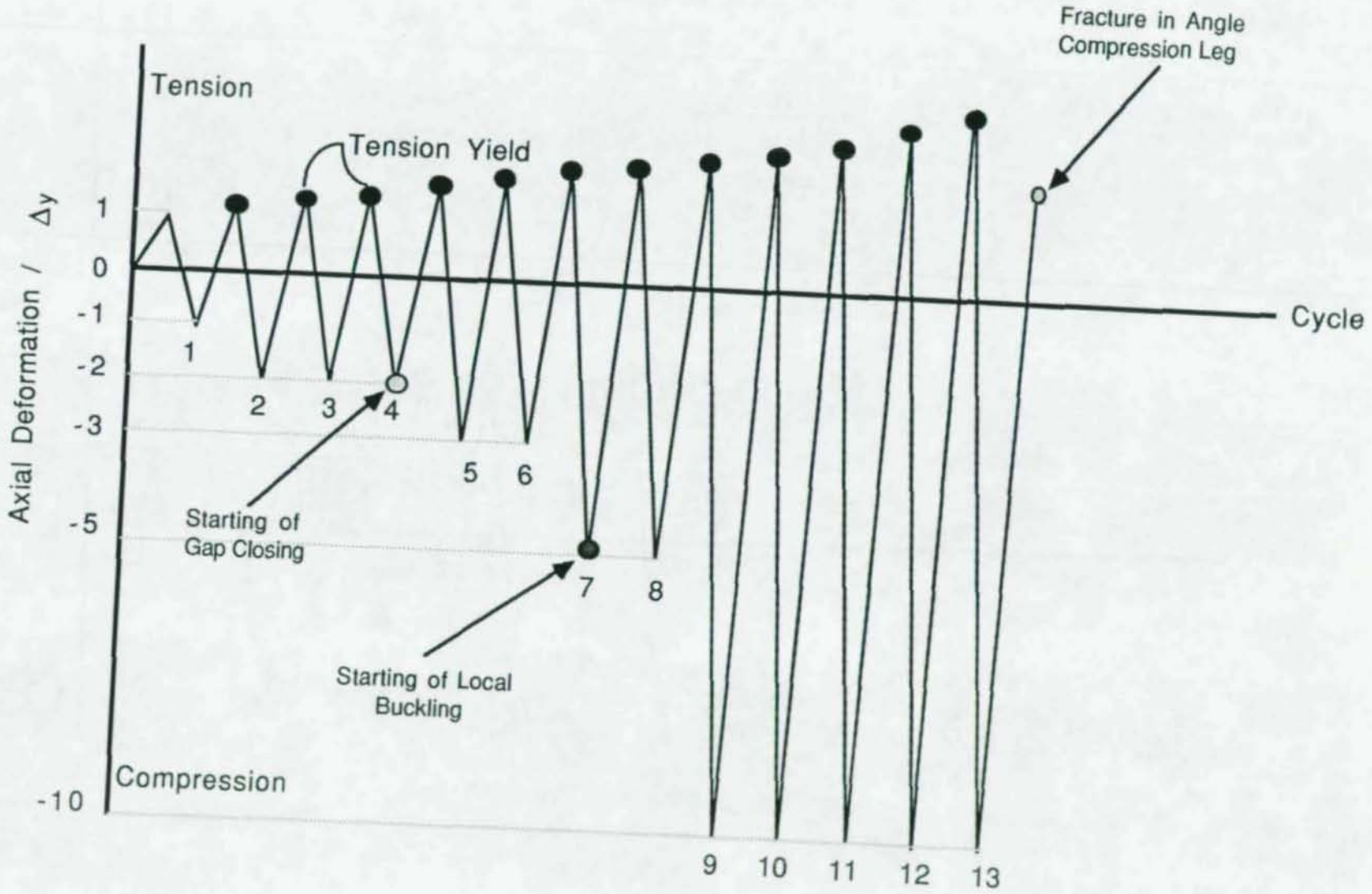

Figure 3.3 - Loading History and Major Aspects of the Behavior of Specimen A3

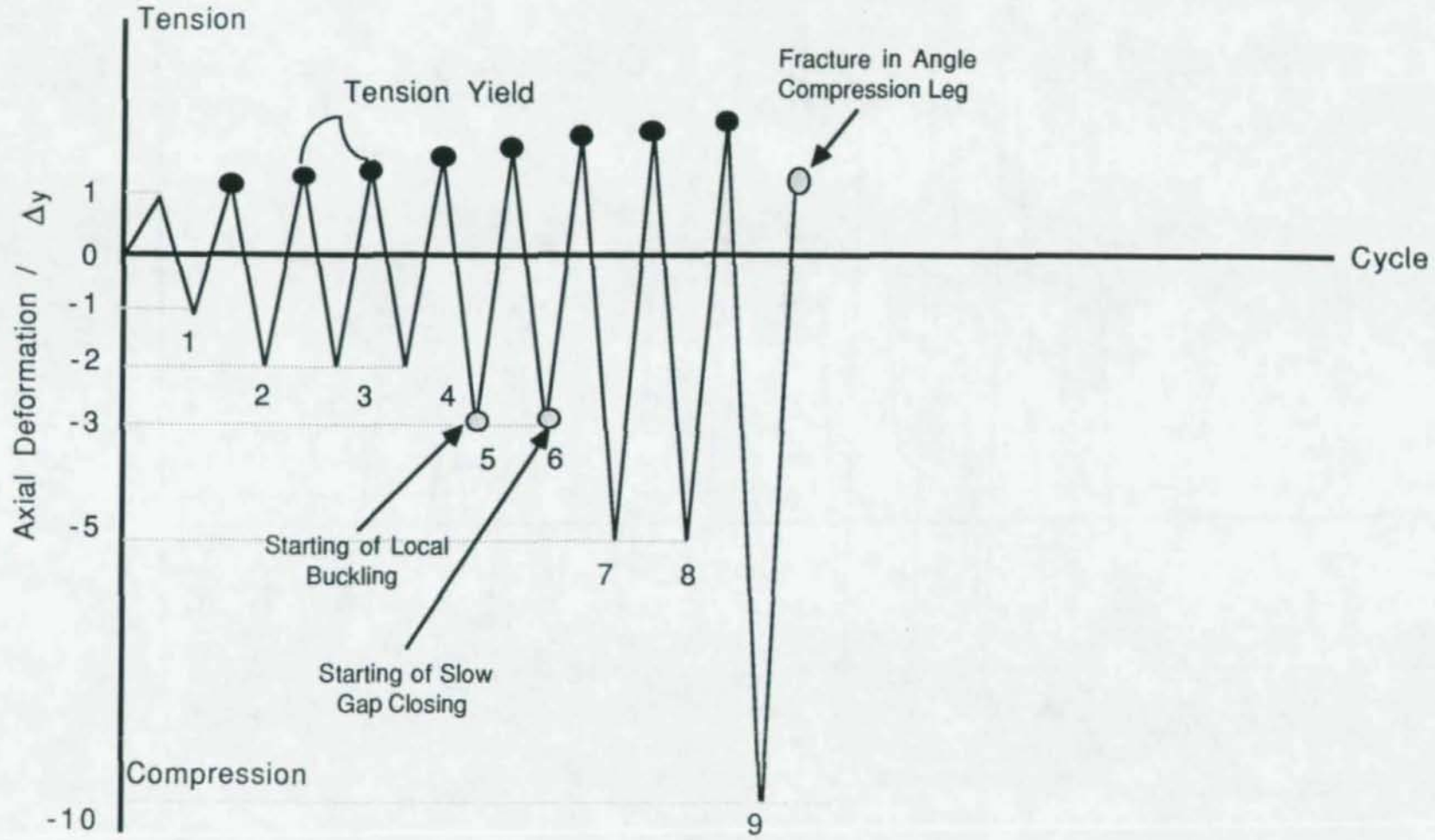

Figure 3.4 - Loading History and Major Aspects of the Behavior of Specimen A4

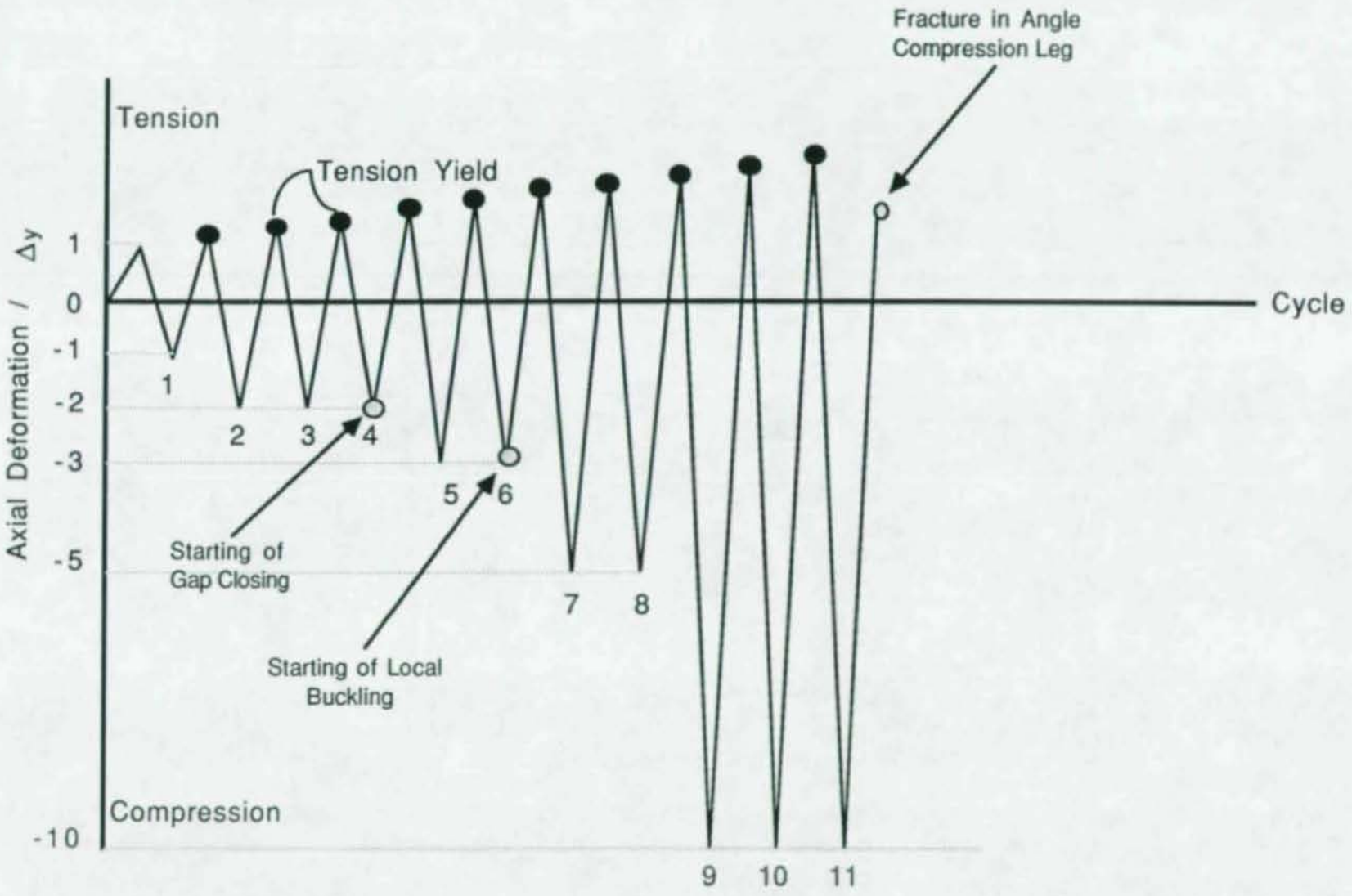

Figure 3.5 - Loading History and Major Aspects of the Behavior of Specimen A5

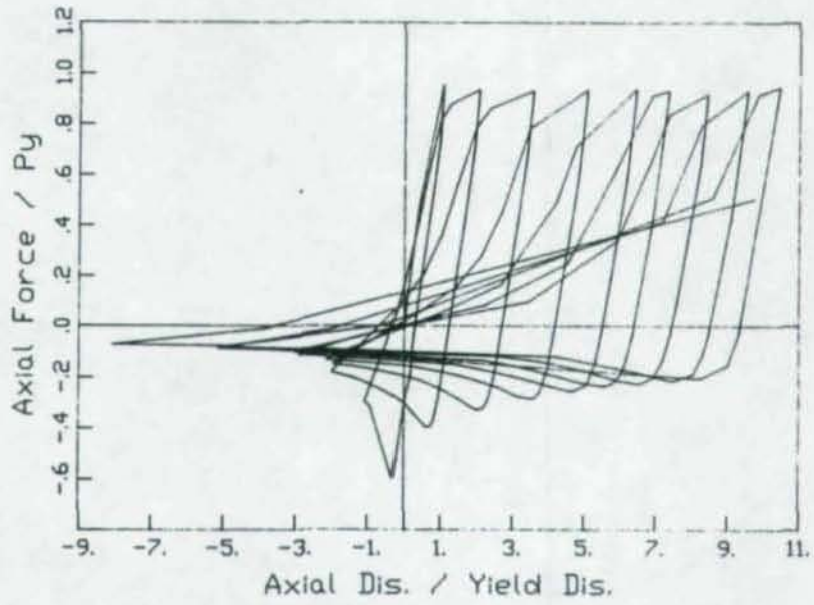

(a) Specimen A4

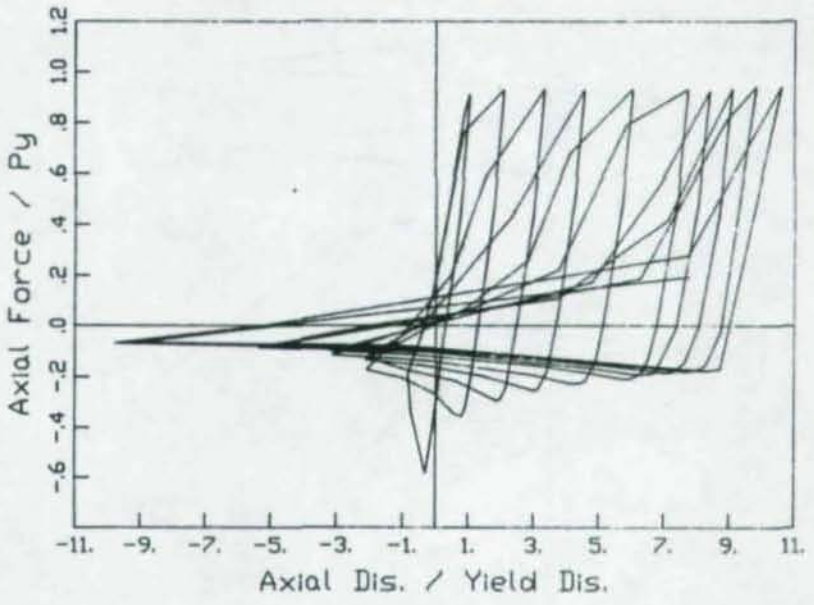

(b) Specimen A5

Figure 3.6 - Hysteresis Loops of Specimens A3 and A4

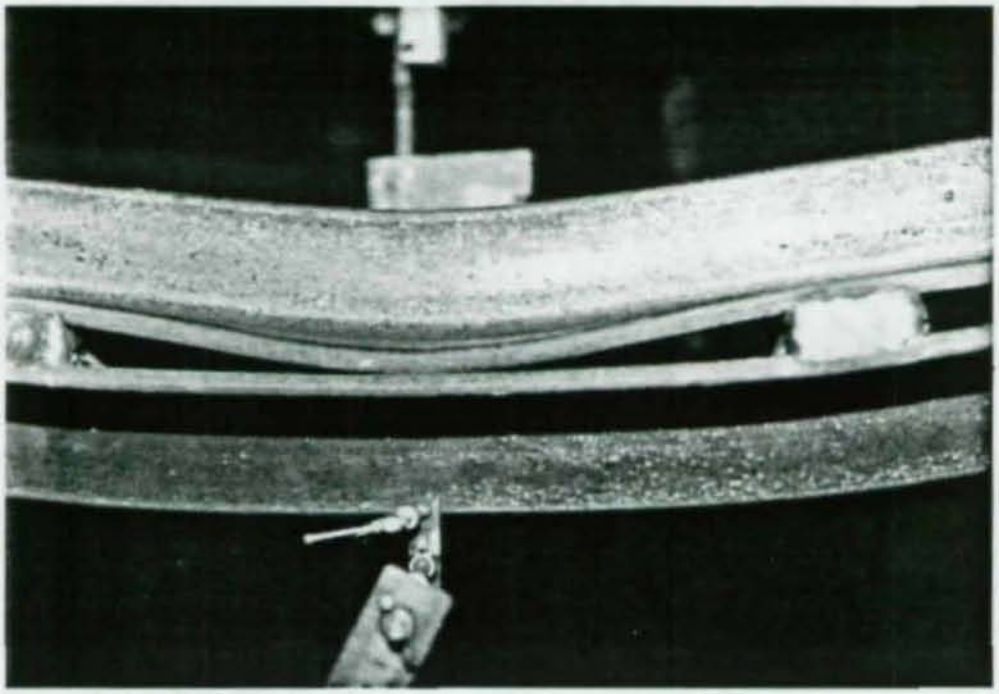

(a) Complete Gap Closing at Bottom While Open at Top

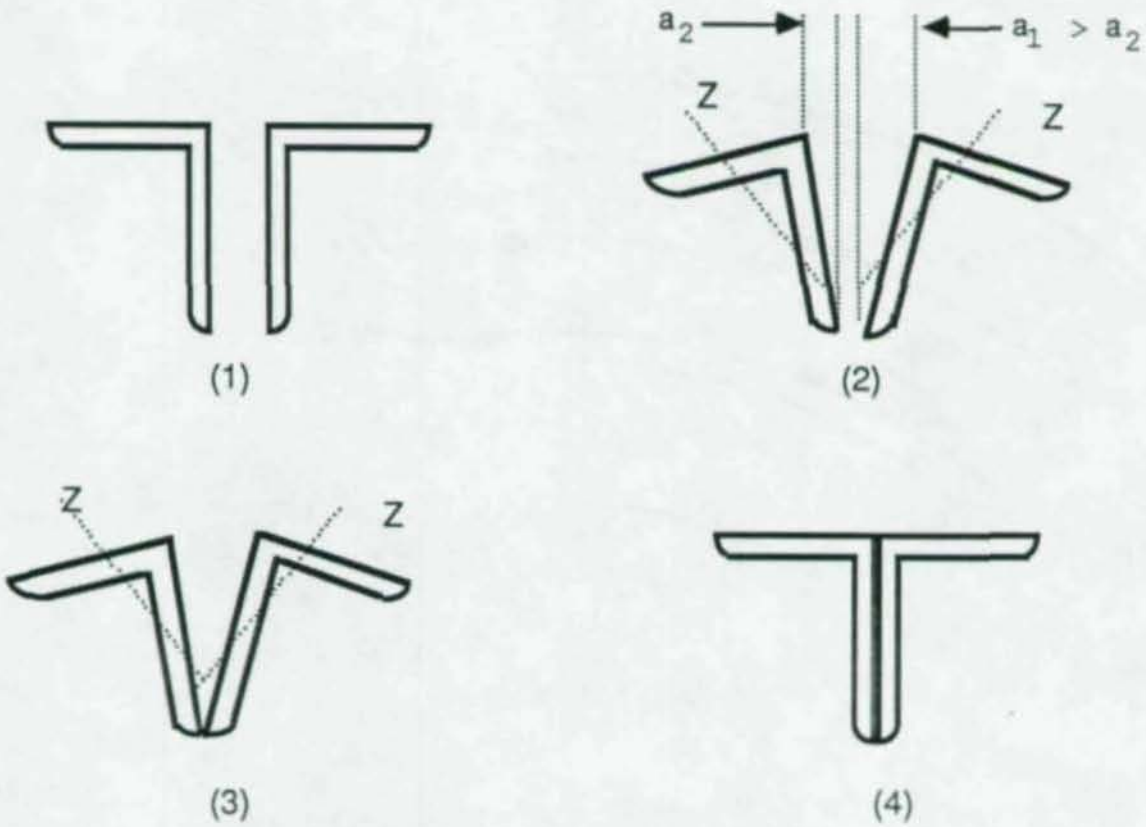

(b) Schematic of the Procedure

Figure 3.7 - Individual z-axis Bending of the Angle Components During Closing of the Gap

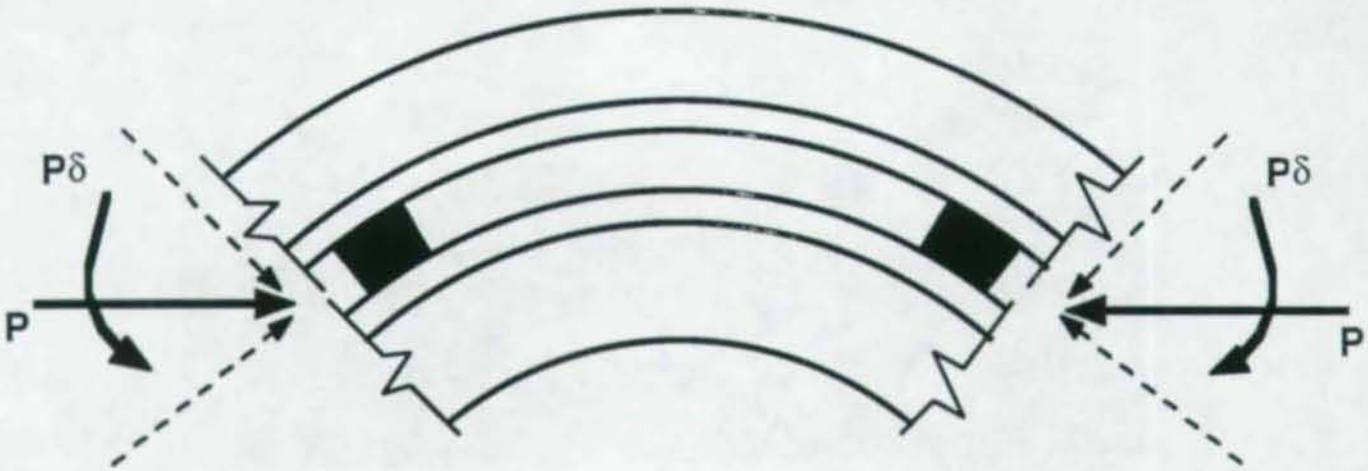

(b) Overall Bending

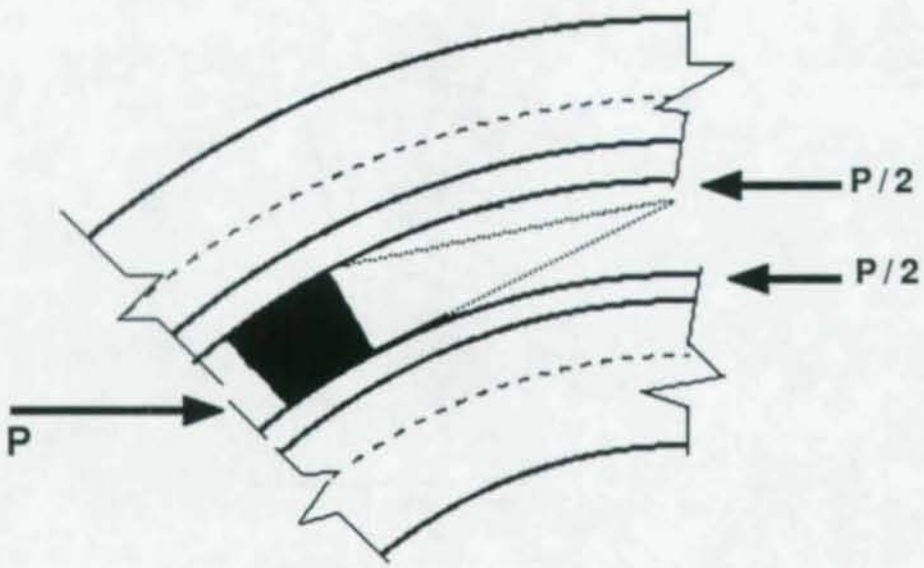

(a) Local Bending

Figure 3.8 - Mechanism of the Gap Closing Between Two Stitches.

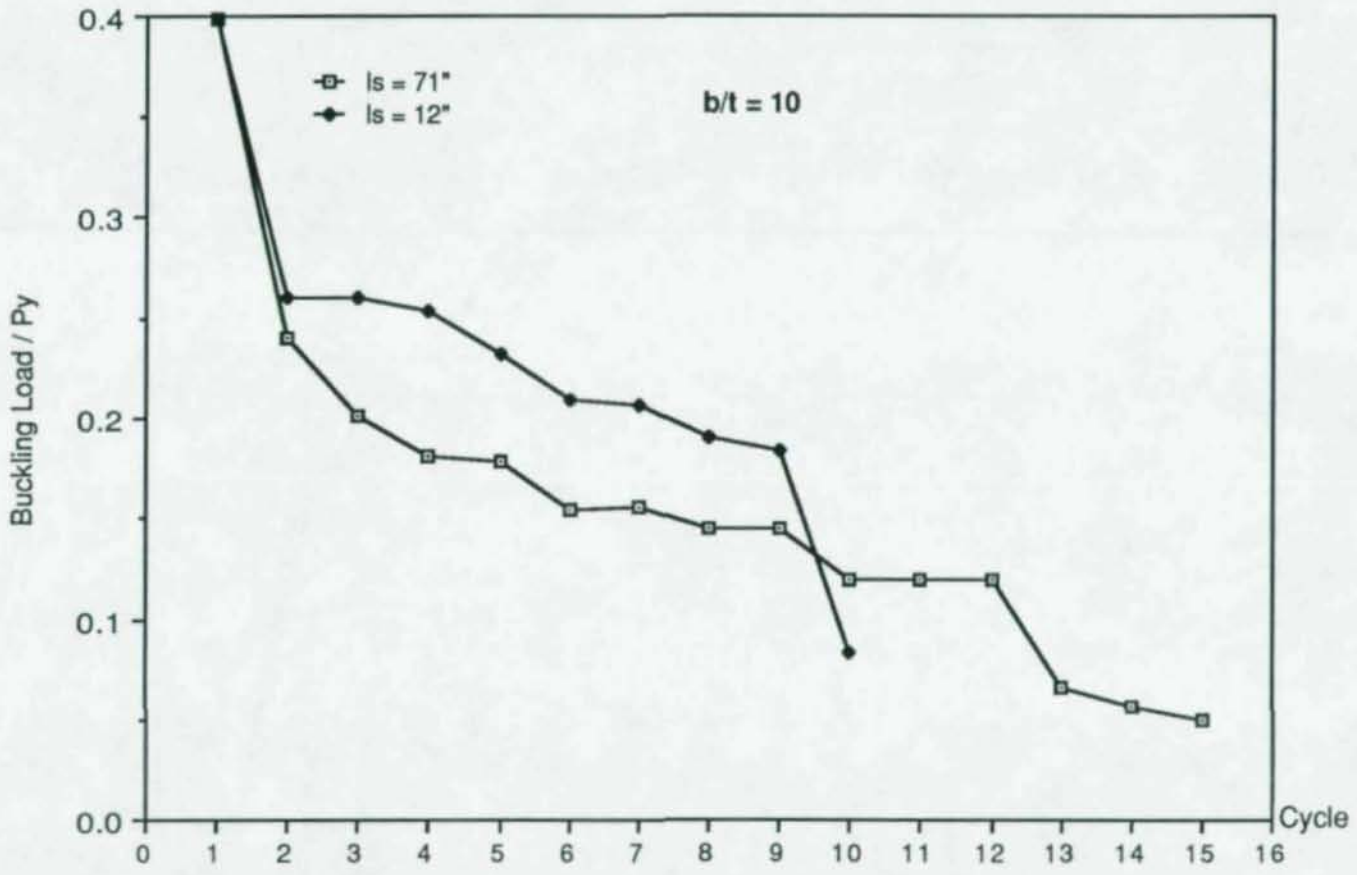

Figure 3.9 - Normalized Buckling Loads of Specimens A1 and A2

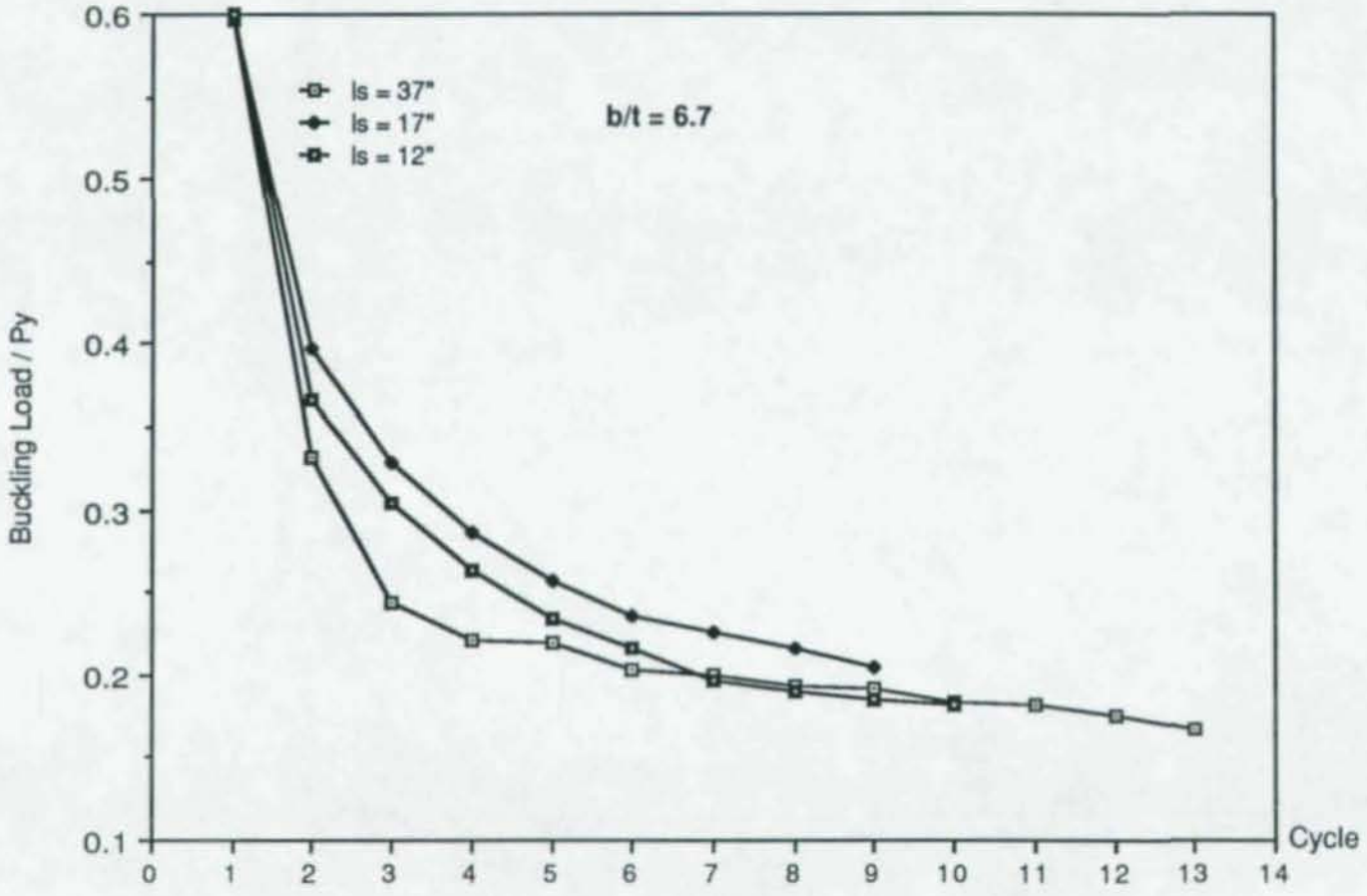

Figure 3.10 - Normalized Buckling Loads of Specimens A3, A4, and A5

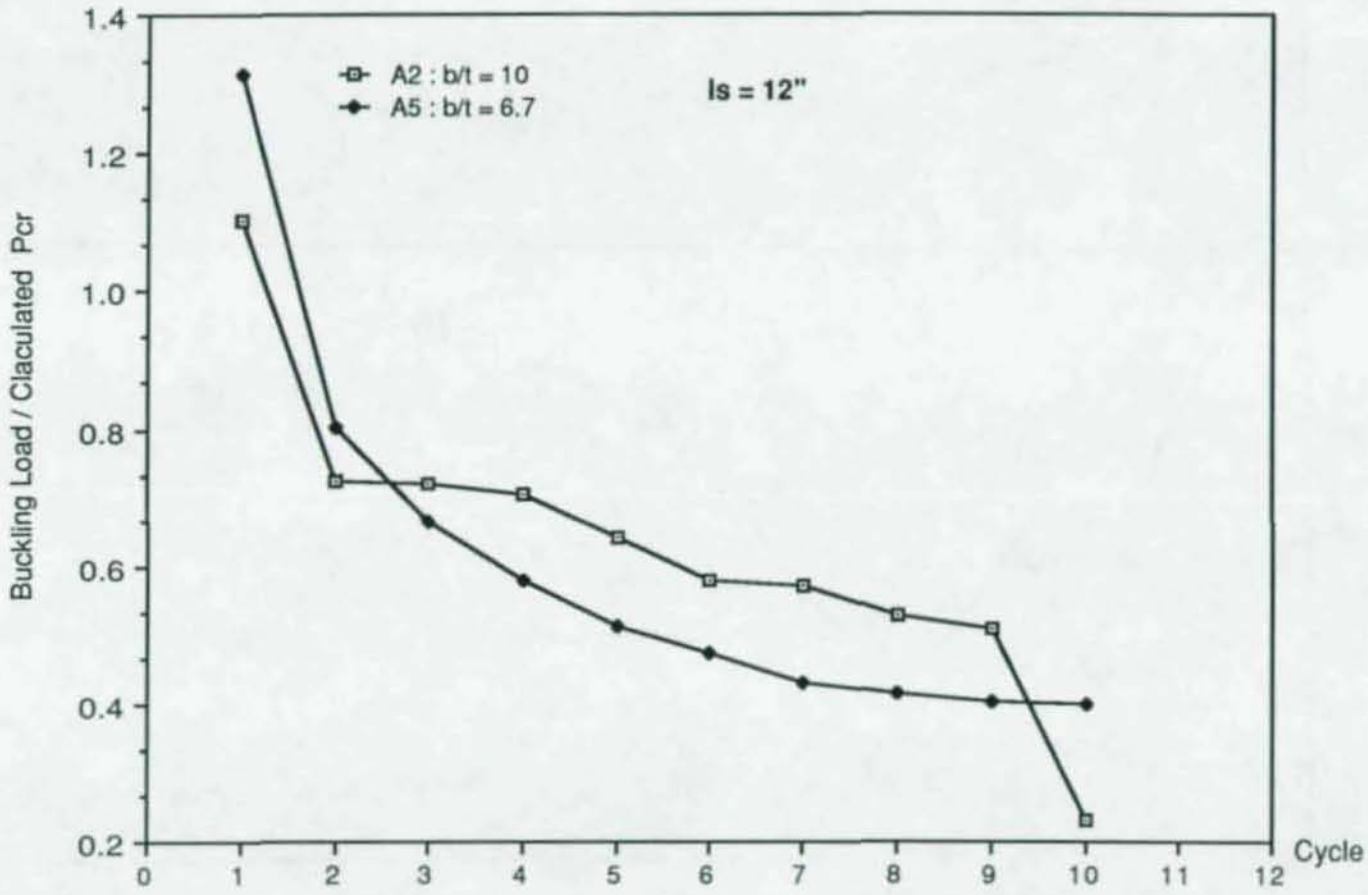

Figure 3.11 - Normalized Buckling Loads of Specimens A2 and A5

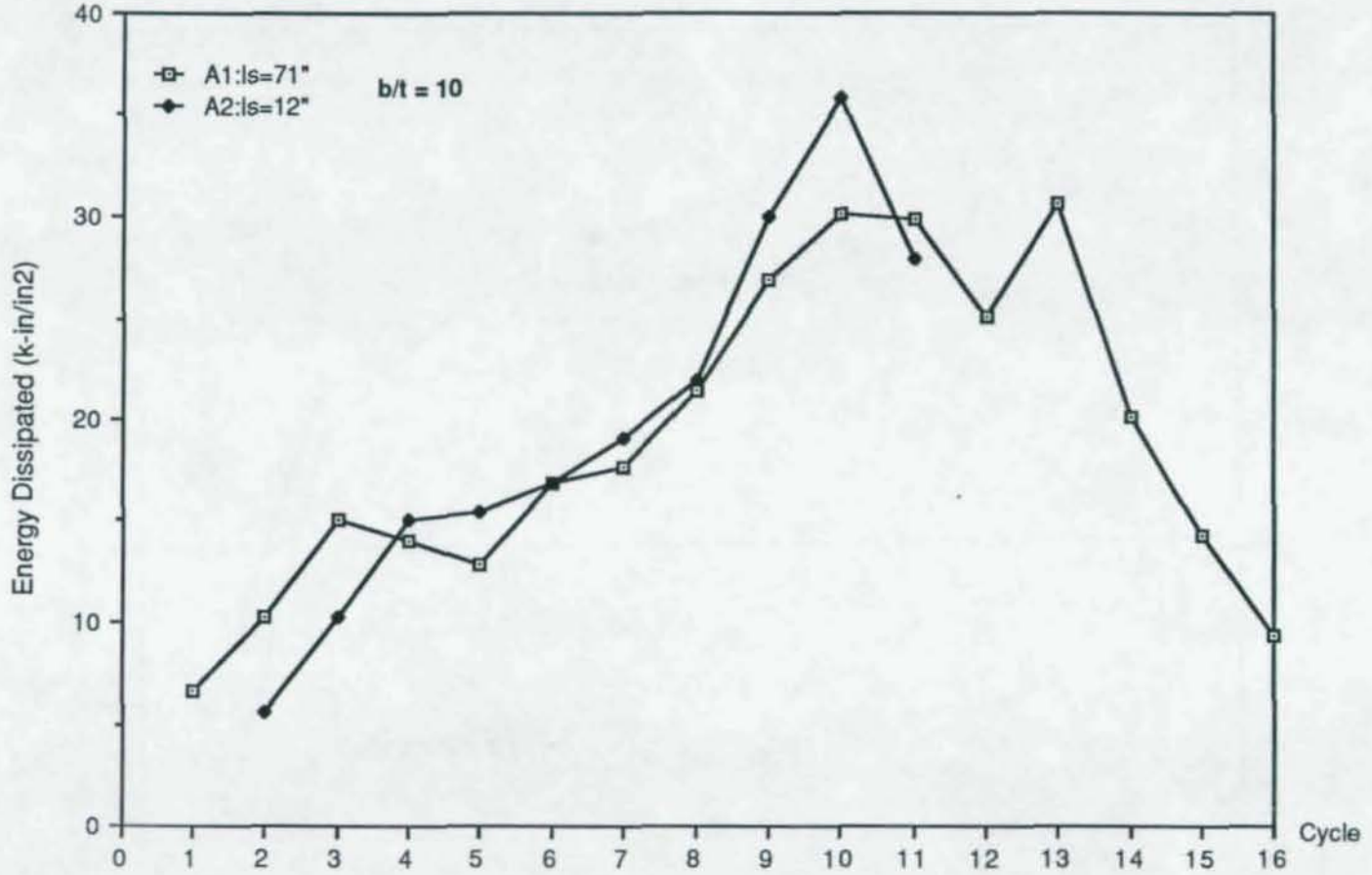

Figure 3.12 - Energy Dissipated Per Unit Area of Specimens A1 and A2

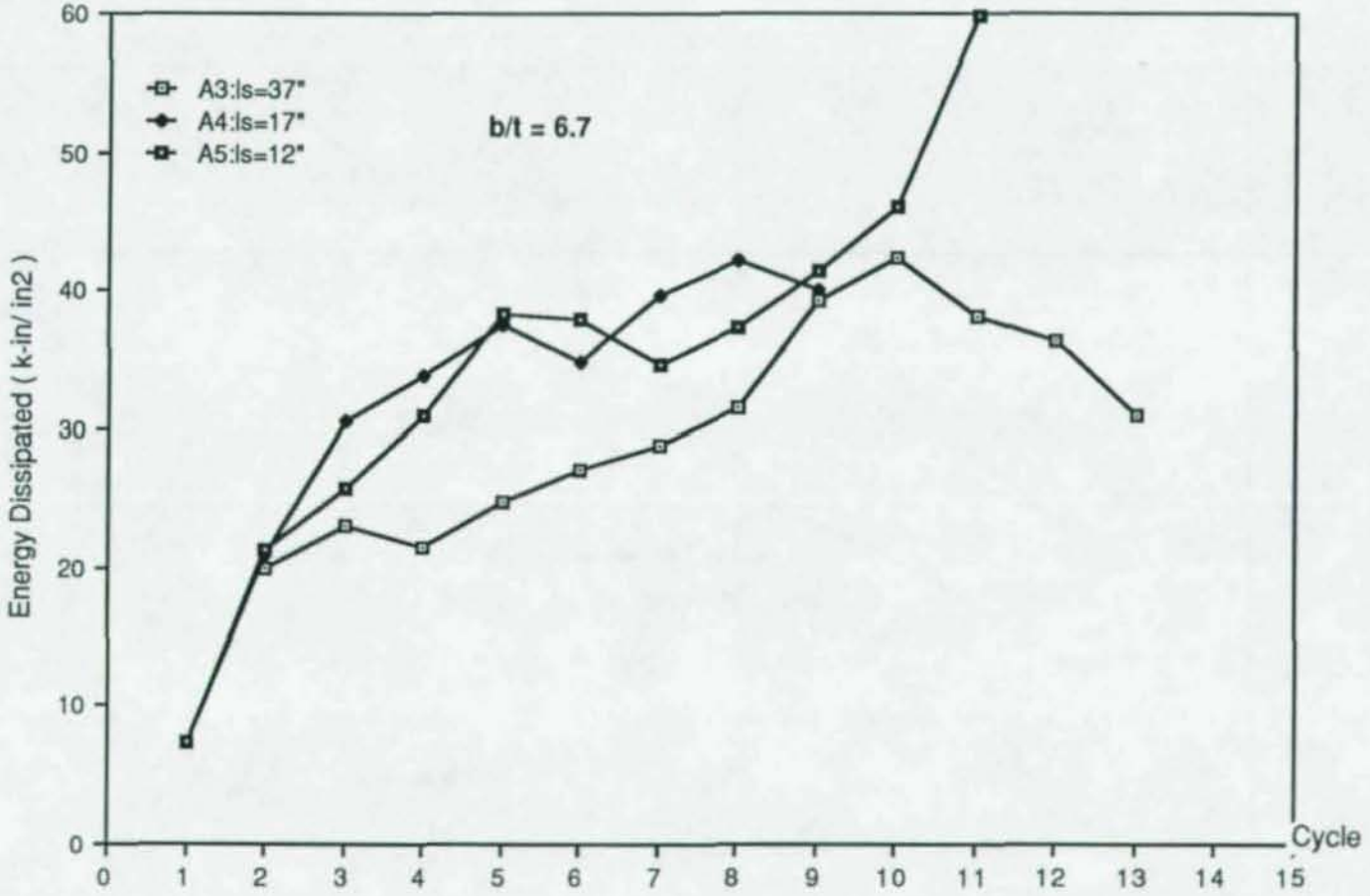

Figure 3.13 - Energy Dissipation Per Unit Area of Specimens A3, A4, and A5

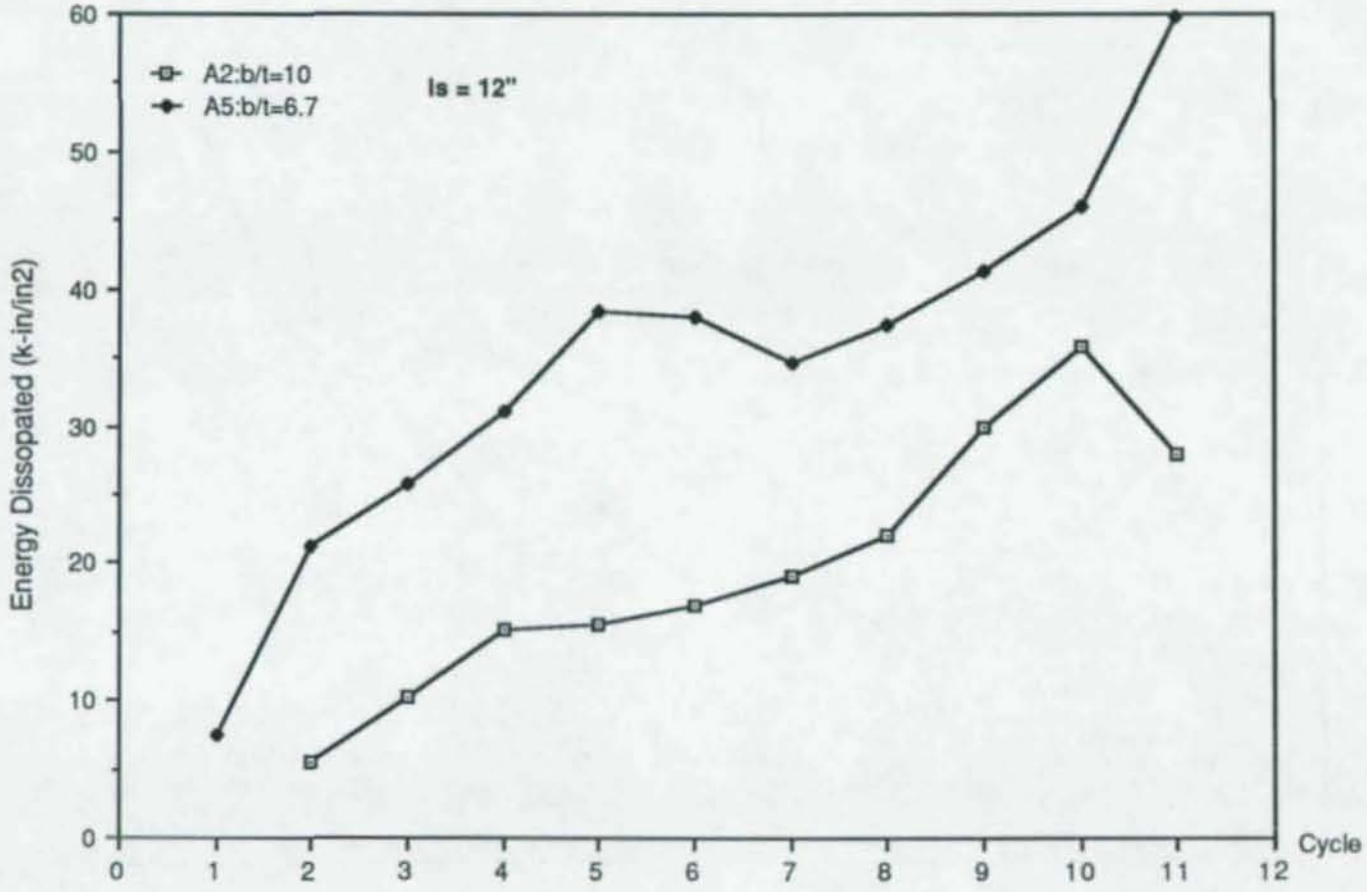

Figure 3.14 - Energy Dissipated Per Unit Area of Specimens A2 and A5

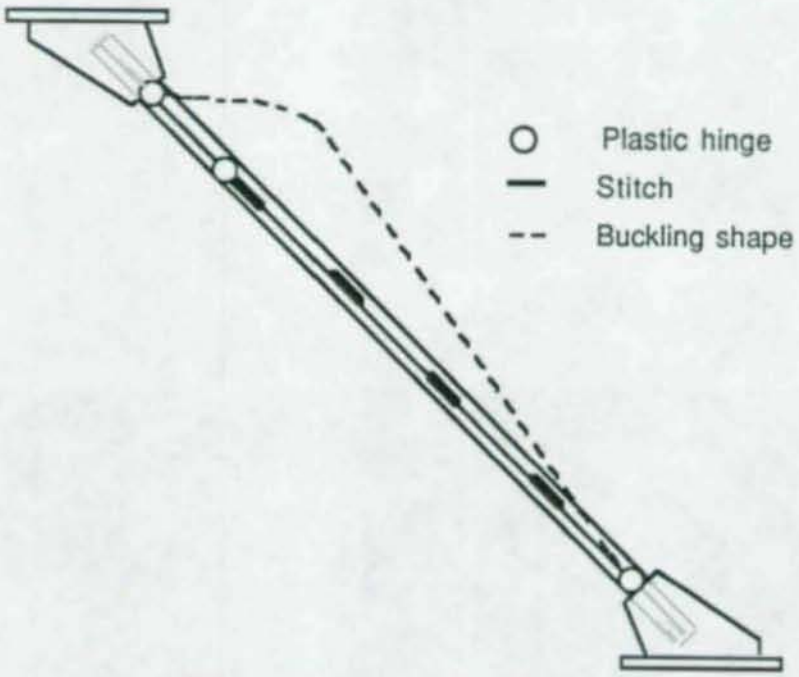

(a) Locations of Plastic Hinges in Specimen C1

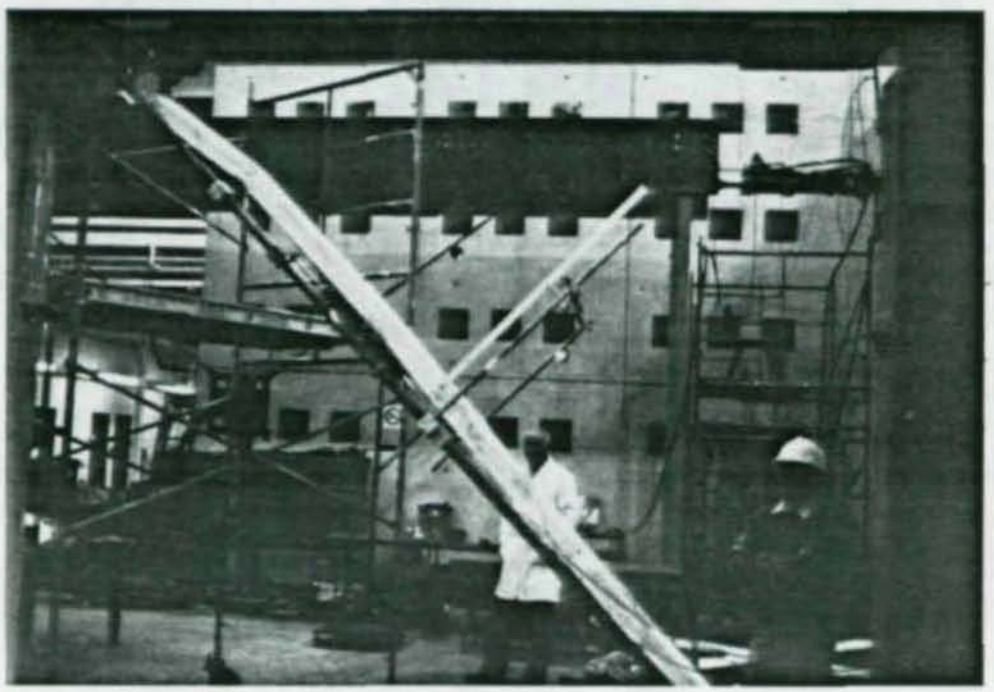

(b) Buckling Shape of Specimen C1

Figure 3.15 - Buckling Shape and the Locations of Plastic Hinges of Specimen C1

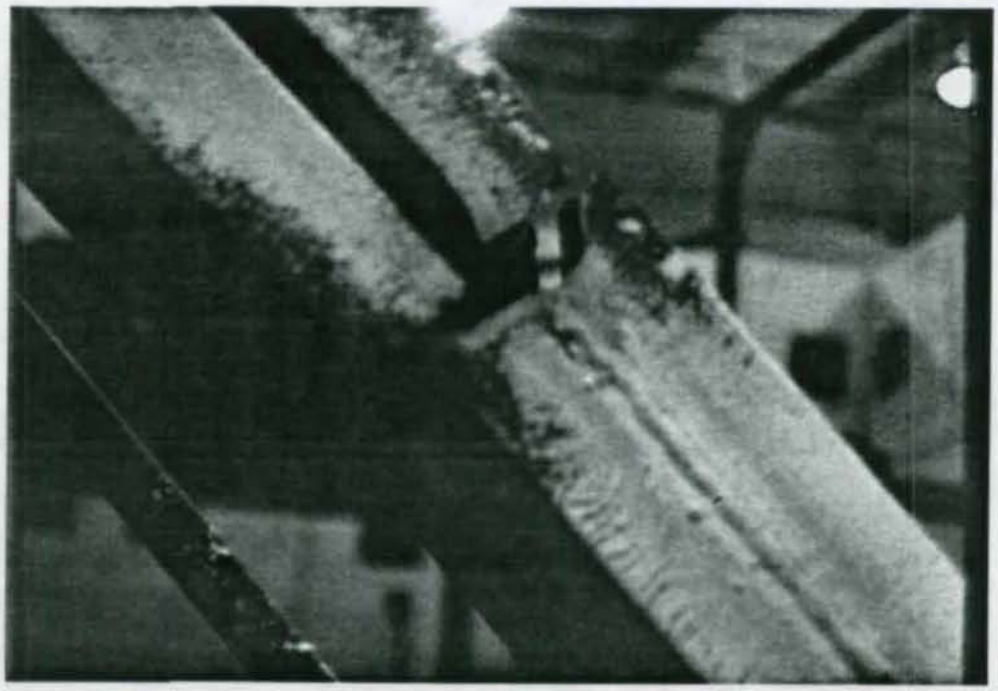

Figure 3.16 - Failure of Specimen C1 in Cycle 3

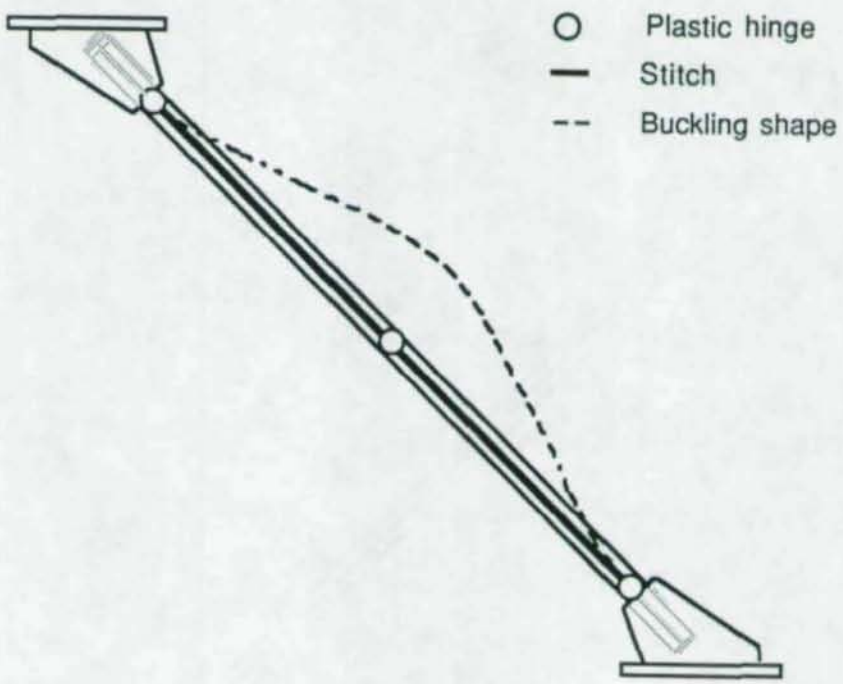

Figure 3.17 - Buckling Shape and the Locations of the Plastic Hinges of Specimen C2

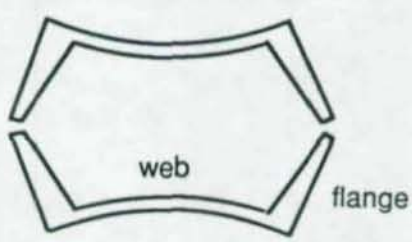

Figure 3.18 - Distortion of Double Channels Section at the Post-Buckling Range

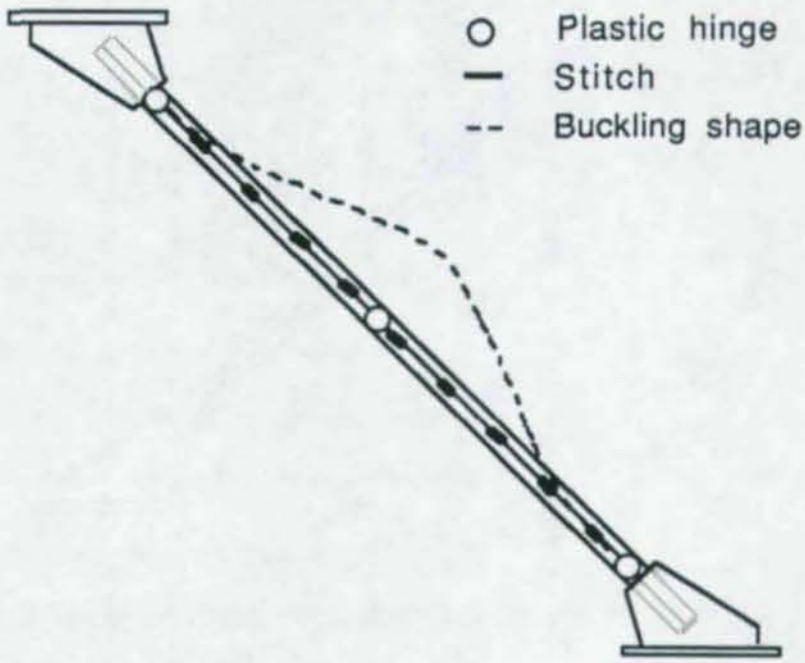

Figure 3.19 - Buckling Shape and the Locations of the Plastic Hinges of Specimen C3

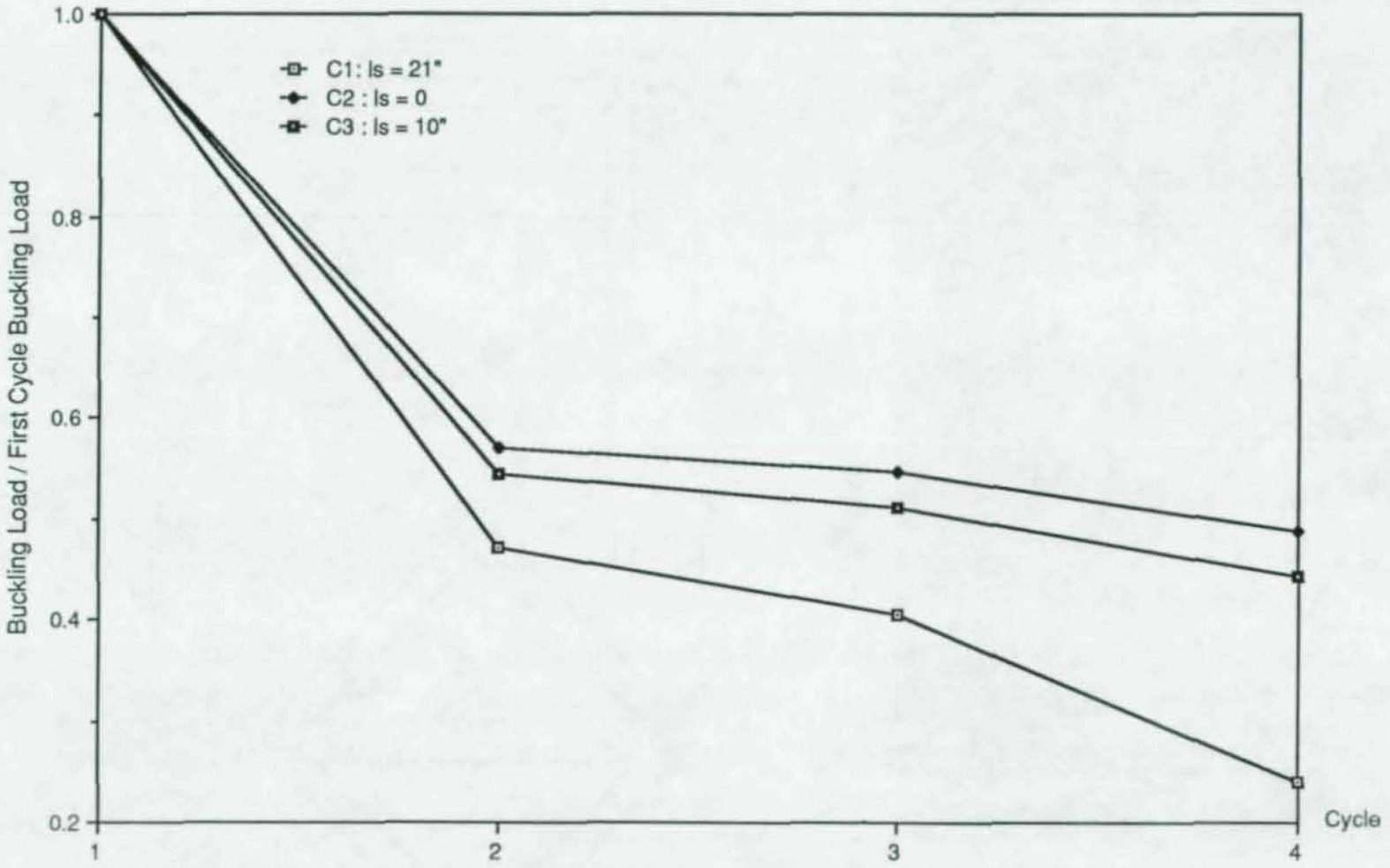

Figure 3.20 - Normalized Buckling Loads of Specimens C1, C2, and C3

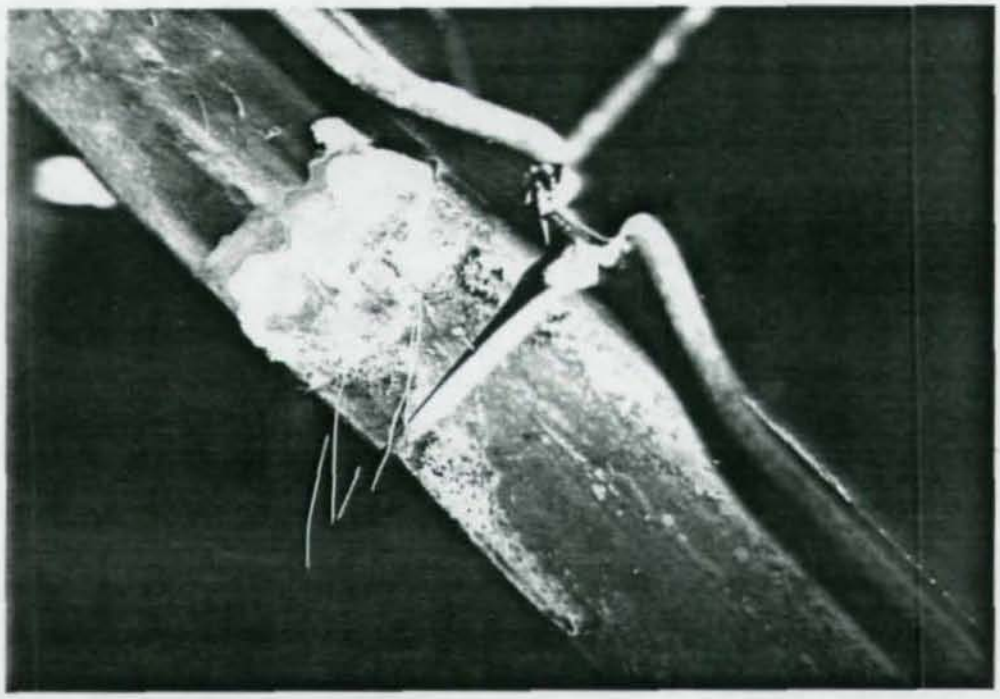

Figure 4.1 - Failure Mode of Double Angle Specimens

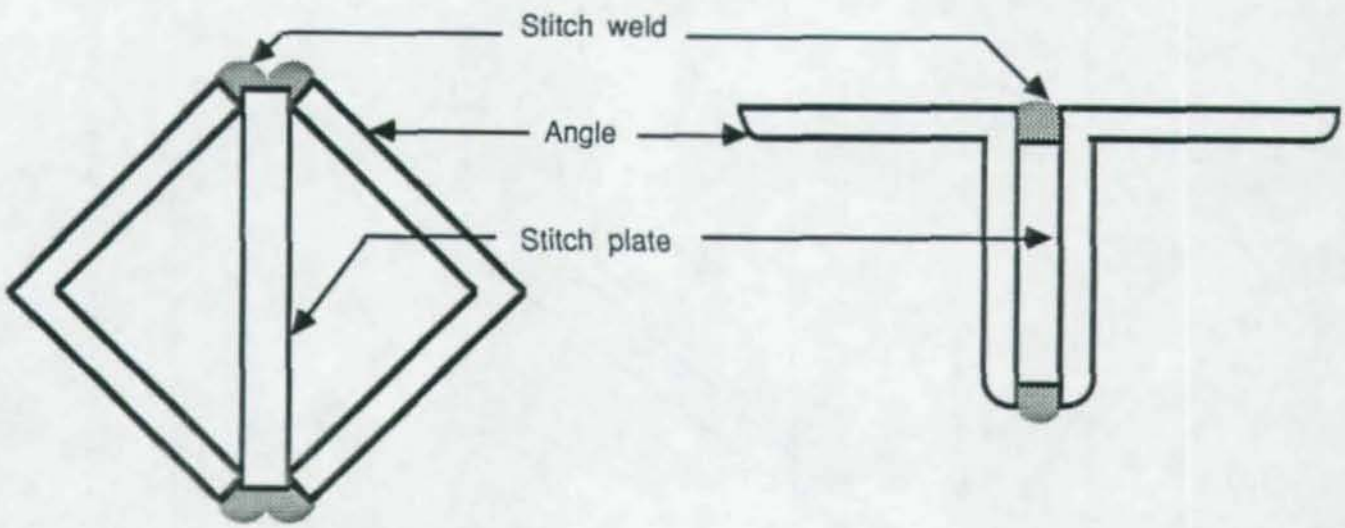

(a) Proposed Configuration

(b) Conventional Configuration

Figure 5.1 - Double Angle Section Configuration